crystals

MDPI

Review

Layered Double Hydroxides: A Toolbox for Chemistry and Biology

Giuseppe Arrabito [1,*], Aurelio Bonasera [1], Giuseppe Prestopino [2,*], Andrea Orsini [3], Alessio Mattoccia [2], Eugenio Martinelli [4], Bruno Pignataro [1] and Pier Gianni Medaglia [2]

1 Department of Physics and Chemistry Emilio Segrè, University of Palermo, 90128 Palermo, Italy
2 Department of Industrial Engineering, University of Rome "Tor Vergata", 00133 Rome, Italy
3 Università degli Studi Niccolò Cusano, Via Don Carlo Gnocchi, 3, 00166 Rome, Italy
4 Department of Electronic Engineering, University of Rome Tor Vergata, 00133 Rome, Italy
* Correspondence: giuseppedomenico.arrabito@unipa.it (G.A.); giuseppe.prestopino@uniroma2.it (G.P.)

Received: 20 June 2019; Accepted: 13 July 2019; Published: 15 July 2019

Abstract: Layered double hydroxides (LDHs) are an emergent class of biocompatible inorganic lamellar nanomaterials that have attracted significant research interest owing to their high surface-to-volume ratio, the capability to accumulate specific molecules, and the timely release to targets. Their unique properties have been employed for applications in organic catalysis, photocatalysis, sensors, drug delivery, and cell biology. Given the widespread contemporary interest in these topics, time-to-time it urges to review the recent progresses. This review aims to summarize the most recent cutting-edge reports appearing in the last years. It firstly focuses on the application of LDHs as catalysts in relevant chemical reactions and as photocatalysts for organic molecule degradation, water splitting reaction, CO_2 conversion, and reduction. Subsequently, the emerging role of these materials in biological applications is discussed, specifically focusing on their use as biosensors, DNA, RNA, and drug delivery, finally elucidating their suitability as contrast agents and for cellular differentiation. Concluding remarks and future prospects deal with future applications of LDHs, encouraging researches in better understanding the fundamental mechanisms involved in catalytic and photocatalytic processes, and the molecular pathways that are activated by the interaction of LDHs with cells in terms of both uptake mechanisms and nanotoxicology effects.

Keywords: layered double hydroxides; cellular biology; catalysis; DNA; drug delivery; hydrotalcite; osteogenesis; photocatalysis; RNA.

1. Introduction

Nanostructured materials or nanomaterials (NMs) represent an important area of research and a technological sector with full expansion for many different applications. They have long been considered of paramount importance due to their tunable physicochemical properties such as melting point, wettability, electrical and thermal conductivity, catalytic activity, light absorption, and scattering, which ultimately result in better performance compared to their bulk counterparts. In general, NMs are described as materials with length of 1–100 nm in at least one dimension, and can be roughly classified according to their:

i) *Composition* (carbon-based, inorganic-based, organic-based, composite),
ii) *Dimension (0D, 1D, 2D, 3D),*
iii) *Origin* (natural, synthetic),
iv) *Synthesis method* (top-down, bottom-up/self-assembly).

Of particular importance is the classification according to their size [1]. *0D nanomaterials* are systems that are at nanoscale in all their *x*, *y*, *z* sizes. Remarkable examples include carbon nanodots [2] and metallic nanoparticles (NPs) [3]. *1D nanomaterials* have one dimension greater than nanoscale, e.g., length on the micron scale in one direction only (for instance carbon nanotubes [4], silicon nanowires [5], or ZnO nanowires [6,7]). They have shown important applications as it both interconnects and has key units with a nanoscale dimension in electronics and optoelectronics. On the other hand, *2D nanomaterials* have at least two dimensions on the micron scale: Examples include nanoplatelets and nanoribbons with length or diameter on the micron scale and a nanoscale thickness. In particular, the synthesis and the application of 2D nanomaterials have become a fundamental research area in materials science, due to their many intriguing low-dimensional features that are different from the bulk properties, making them more attractive for subsequent utilization as key building blocks of nanodevices [8]. Besides the basic understanding of new physico-chemical phenomena, 2D NMs are also particularly interesting for investigating and developing novel applications in sensors, photocatalysts, nanocontainers, nanoreactors, and templates for 2D structures of other materials [9]. Three-dimensional nanomaterials (3D) can be defined as materials whose characteristic x, y, z dimensions are well beyond the nanoscale (i.e., >100 nm). These systems are typically not included in the category of nanostructured materials, unless their internal structure is nanostructured. Typical examples of this class of materials are the following: dispersions of nanoparticles, bundles of nanowires, as well as multi-nanolayers, nanocrystalline, or nanoporous materials [10].

Among NMs, layered double hydroxides (LDHs) represent an emerging class of 2D layered materials belonging to the group of hydrotalcite-like (HT) compounds, or anionic clays [11]. LDH structure can be described based on the stacking of charged brucite-like layers consisting of a divalent metal ion M^{2+} (e.g., Ca^{2+}, Zn^{2+}, Mg^{2+}, Ni^{2+}), octahedrally coordinated to six OH^- hydroxyl groups, in which part of the divalent cations (M^{2+}) are substituted by the trivalent ions M^{3+} (e.g., Al^{3+} Fe^{3+}, Cr^{3+}, In^{3+}). Such replacement leads to the formation of positively charged layers, whose net charge is compensated, to maintain the global electroneutrality, by the presence of exchangeable anions (A^{n-}, such as hydroxyl groups, nitrates, carbonates, and sulfates) in between the layers conjointly with water molecules. The general formula of LDHs is the following: $[M_{1-x}{}^{2+}\ M_x{}^{3+}(OH)_2]^{x+}\cdot[A_{x/n}]^{n-}\cdot mH_2O$, where M^{2+} and M^{3+} are the divalent and trivalent metal ions, respectively, A^{n-} are inorganic or organic anions, m is the number of interlayer water, and $x = M^{3+}/(M^{2+}+M^{3+})$ is the layer charge density, or molar ratio. LDHs are characterized by a low dimensional opened structure that is suitable for physico-chemical intercalation and adsorption processes with a large variety of molecules ranging from organic molecules to biomacromolecules.

The conventional approach to the synthesis of LDHs is based on the coprecipitation method [12–14], which can be briefly described as follows. The addition of a base to a water solution containing the salts of two different metals, namely M^{2+} and M^{3+}, causes the precipitation of the metal hydroxides and the formation of LDHs. The precipitates are collected, washed and then dried to be deposited on a solid substrate, or dispersed in solution phase. In some applications it is necessary to produce homogenous films onto solid substrates [15,16]. For this, two different research groups [17,18] demonstrated the possibility of growing stable films of well-formed interconnected LDH nanoplatelets directly onto aluminum surfaces, by immersing aluminum thick foils in a water solution of zinc nitrate or acetate. Differently from the conventional growth method, a single salt is employed in the growth solution providing the divalent metal (Zn^{2+}), while the trivalent ion (Al^{3+}) is provided by the sacrificial aluminum foil, which behaves as both reactant and substrate, finally improving the adhesion as well. In this regard, the growth of regular ZnAl LDH nanoplates [19] on Al-coated silicon substrates was demonstrated, along with the influence of the reacting aluminum layer thickness on the final morphology and composition of the LDH nanostructures. These kind of LDHs found application as gas sensors [20], Li-ion battery electrodes [16], for enhanced oxygen evolution catalysis [21], and surface enhanced fluorescence [22]. LDH systems are subjected to the so-called "memory effect", i.e., for suitably low calcination temperatures, the resulting phase can be restored to that of LDH by

rehydration in water. Remarkably, during the rehydration new anionic species can be intercalated and functionalized, obtaining desired physicochemical properties [23]. In the following, the M^{2+}:M^{3+} stoichiometric ratio in LDH will be precisely mentioned and discussed, only if definitely stated by the authors to be meaningful for the application of the LDHs. Otherwise, the LDH formula will be simply indicated as $M^{2+}M^{3+}$ LDH (see Figure 1).

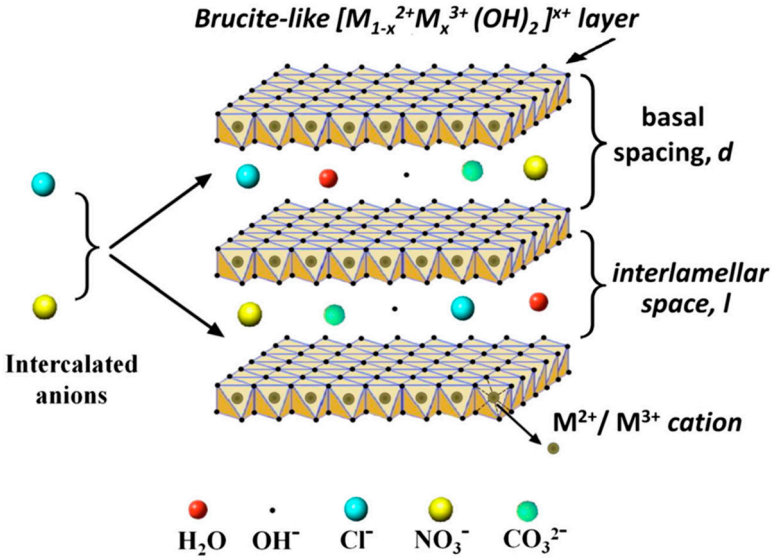

Figure 1. Schematic view of the $M^{2+}M^{3+}$ LDH general structure, with Cl^-, NO_3^- and CO_3^{2-} anions intercalated in the brucite-like structure. Other possible chemical species eventually present in the interlamellar space are reported, i.e., hydroxyl groups and interlayer water molecules. The figure is reprinted from Ref. [24] under a Creative Commons Attribution Non-Commercial No Derivatives License (CC BY-NC-ND).

The aim of this review is to introduce the emerging role of LDH materials in chemistry and biology, providing the reader with a broad up-to-date view of the role of these materials in these fields. Indeed, given the widespread contemporary interest in these issues, the topic is certainly hot, and from time-to-time, it is necessary to review the recent progresses. Differently to the previously published reviews, the aim of the present work is to provide some fundamental references concerning earlier investigations and also providing recent researches that are establishing new trends. As to the chemistry-related topics, the interest for LDHs is reviewed especially focusing on relevant organic chemistry reactions and recent advances in photocatalysis, with the ultimate goal to elucidate the key role of LDHs that is rarely investigated in literature. As to the biology-related field, LDHs are reviewed focusing within the well-explored applications in electrochemical and optical biosensors, along with DNA delivery. In addition to these, the review summarizes novel and barely explored topics, namely optical sensors, RNA delivery, cellular differentiation, and fundamental biological pathways relevant to the LDHs uptake into cells. The critical and unprecedented overview provided by the present review is hopefully able to motivate new researchers interest in these emerging fields.

Initially, we will discuss the immense potentiality of these 2D materials in organic chemistry, in particular focusing on their role as catalysts in highly relevant chemical reactions, namely the Baeyer–Villiger reaction, Knoevenagel reaction, Michael addition, and transesterification (Section 2). We will then focus on the outstanding role as photocatalytic centers, discussing their applications to organic molecule degradation, water splitting reaction, CO_2 conversion/reduction, and other examples (Section 3). Subsequently, we will analyze the intriguing role of these materials in biology, where their biocompatibility and the suitability as powerful drug vectors have triggered an enormous research interest in the last few years (more than 1000 papers published in 2018 regarding drug and DNA delivery, according to data extracted from the Scopus database). In this regard, we will provide a focus

on the research results of the last two years, regarding applications of LDHs as biosensors (Section 4), especially focusing on the novel exciting applications as optical sensors. We will then analyze their important role as nucleic acid delivery agents (Section 5), providing an unprecedented view on the novel applications in siRNA therapy. Lastly, a specific view on LDHs as key materials in cellular differentiation, drug delivery, and contrast agents will also be provided (Section 6).

2. LDH Applications in Organic Catalysis

This section will focus on the role of LDH-based materials in organic chemistry, mainly as catalyst for the preparation of fine chemicals, intermediates, and valuable molecules. The interest for LDHs in chemical synthesis is due to some common features they share with classic heterogeneous catalysts; once a reaction has been catalyzed by LDHs, these layered materials can be easily removed from the crude reaction mixture (e.g., by filtration) and recovered for next reaction cycles, with significant simplification of the work-up procedure for the chemist. Among the plethora of available heterogeneous catalysts, LHDs have some additional appealing features, such as the simplicity of their preparation from cheap precursors, the involvement of non-harmful precursors, low toxicity of their possibly produced decomposition products, and no need of expensive rare elements. For details on synthesis routes, the reader is advised to go back to the previous Section, however some other aspects relevant to LDH fabrication strategies will be briefly discussed here as well, in order to clarify why scientists devote increasing attention towards specific LDH compounds.

Chemists' interest over clays does not go so back in time: early in the 80s the works of Kruissink and Reichle on methanation [25] and acetone oligomerization [26], respectively, pointed out that LDHs could be employed as precursors for catalytic species, after thermal degradation. In those works, the properties of the pristine LDHs were not addressed, but shortly after Martin and Pinnavaia revealed how LDHs could be useful also in their pristine form [27]. From there on, the number of publications on catalytic LDHs quickly grew. The aforementioned paper not only had a historical relevance, but it allows us to discuss the different strategies that researchers have when dealing with LDHs as catalysts (see Figure 2):

i) *LDH-materials as supporting surface*. The insertion of new species adds a reactivity that pristine LDHs do not possess at all. LDHs role lies in the chemical confinement, enhancement of catalyst selectivity, but no active participation to the reaction steps,
ii) *LDH-materials as source of catalytically active species*. LDHs are induced to transform in a new material with the required catalytic properties,
iii) *LDH-materials as absorbers*. The catalytic species are adsorbed in between the interlayer galleries, and can be lately exchanged with the external environment. LDHs must be previously exposed to an excess of the species to be adsorbed, which are lately released. It is evident that in this case, LDHs act as a reservoir, or create a catalytic environment/condition, but the active role is due to another atomic/molecular object,
iv) *LDH-materials as they are*. The catalytic properties belong to the lattice as it is, and are not subject to the inclusion of other species.

We are going to restrict our discussion on the latter case. Indeed, in the first case, LDH materials derive their reactivity from the hosted species, and the LDH crystal lattice has a relatively marginal role, boosting up the catalytic activity of the absorbed species but not participating directly. Several reviews have already been published focusing over specific examples where carbon nanoforms [28,29], metal nanoparticles [29,30], organic guests [31,32], and oxometalates [33,34] are used for the preparation of interesting LDH-based hybrids. In the second group, LDHs typically undergo thermal stress, with a consequent loss of structural features and transformation into mixed metal oxides (MMOs) [35,36]. Such a procedure is useful when the lattice is limiting the interaction between the metal centers and the reactants, thus the catalytic behavior arises when the layered clay framework, that is the key feature of a LDH-material, is lost. MMOs are used for a wide range of reactions, mostly in the gas phase [37–40],

and various alkylation protocols, condensations and transesterifications [41]. The easiest way to reduce LDHs into MMOs is calcination, but this procedure should not be considered as a protocol since it points only to the loss of LDH structural features. Firstly, it could be a simple way to remove excess of water, which is detrimental for several catalytic routes [42]. Secondly, operating a strict control over calcination temperature, the so-prepared MMOs can regenerate LDHs after rehydration [43–46]. This is the so-called "memory effect", and published data reported that calcination temperature (T_c) should be below 500 °C, as well as compatible with thermal stability of eventual other species introduced/grafted on LDHs [47].

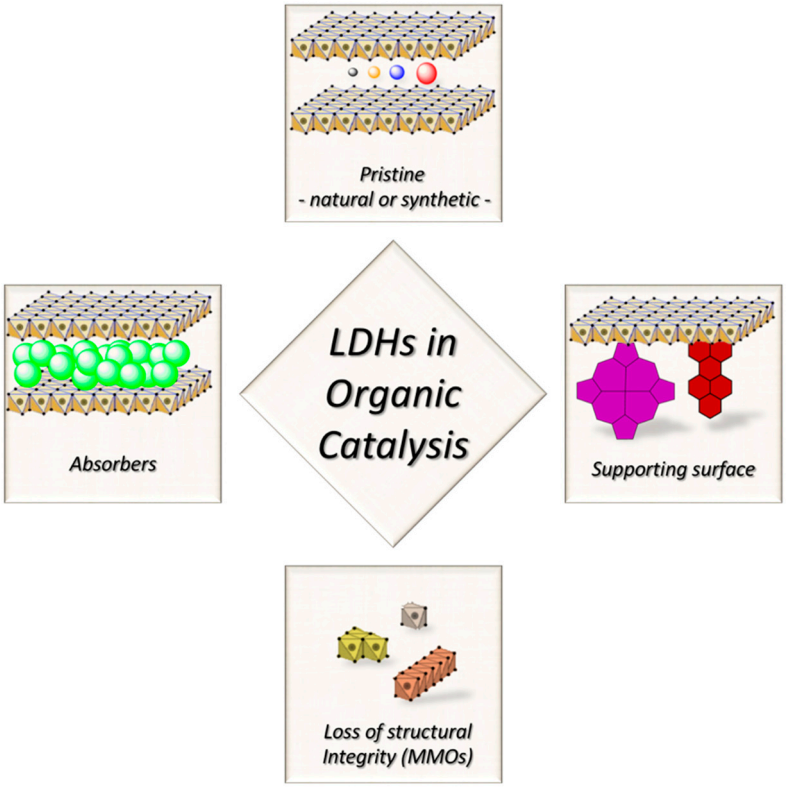

Figure 2. Representation of different possible approaches for the development of LDH-based catalysts for organic synthesis.

The reactivity intrinsically ascribed to LDHs is related to their layered structure formed by cations, anions and structural water molecules, but there are other ruling parameters; the most crucial ones are summarized here:

i) Considerable anion-exchange capability, due to the freedom that anions have to travel through the interlayer aqueous medium, the absence of strong localized interactions and specific steric constrains [48–50],
ii) Pronounced basicity, due to either structural hydroxyl anions (Brønsted theory, hydrated material) and O^{2}–M^{2+} pairs (Lewis theory, water-free calcined material) [51],
iii) Nature of metal cations, presence of more than two metal species within the lattice (see below).

Intriguingly, the metal cation composition strongly contributes to the specific reactivity of LDHs, but it tunes as well the strength of basic moieties. The incorporation of specific metals in the octahedral layer can produce LDH compounds with unexpected and novel properties, as well as modulate the existing chemical reactivity [51,52]. It is worthy to mention literature where the arrangement of cations within the LDH lattice is discussed. As a matter of fact, the ordering of cations is believed to have crucial effects on many of the physicochemical properties of LDHs, affecting the charge density

of the metal hydroxide sheets, and the overall bonding, mobility, orientation, and reactivity of the chemical species in the interlayer spaces and on the surface [53–58]. It is therefore desirable to have homogeneous distribution of cations without segregation of phases with specific composition, which would result in varied reactivity, and in catalytic processes, generation of nonspecific products [59]. Similarly, the composition of the anionic species can be varied [60]. Some other clear advantages bring researchers to consider LDHs as catalysts of choice instead of more traditional ones [57,58]. Besides their activity and/or selectivity, in heterogeneous catalysis LDHs offers the opportunity of minor production of waste and an easier removal of the catalytic species from the crude reaction mixture. One example is given by the work of Lü et al., who fabricated LDH-based catalytic films over porous alumina membrane [61]. Interestingly, the authors revealed superior activity of the catalytic film in the aldol condensation of acetone, compared to the LDH-powders prepared under identical conditions. The authors also pointed out that those LDH-crystallites grown over the alumina support retained hexagonal plate-shape perpendicularly on the substrate, which favored the diffusion of the reactants throughout the substrate, despite the more disordered organization of the LDH-powders.

In the next paragraphs, we will consider some organic reactions of interest, and we will try to give an overview of the most relevant and recent contributions of LDH compounds in organic synthesis. Our aim is to give to the general audience, not only to organic chemists, the feeling why so many researchers focused on specific reaction pathways. We will report, as well, some examples regarding industrially relevant molecules and/or precursors whose synthesis can be improved applying LDHs chemistry. Our attention regards the following classes:

i) Baeyer–Villiger reaction,
ii) Knoevenagel reaction,
iii) Michael addition,
iv) Transesterification (biodiesel production).

We would like to recommend a review by Sels et al. [62], whose analysis embraced several classes of reactions, although the reader should notice that no distinction was made among LDHs, MMOs derived from LDHs, intercalated materials and else. With an insight into life sciences, it is worth to point out that the synthesis of therapeutic molecules (i.e., drugs, active compounds) typically requires a high number of transformation and purification steps. A straightforward strategy to improve the sustainability of complex chemical synthesis is to consider how nature synthesizes biologically active compounds using enzymatic catalysis. Unfortunately, enzymes that catalyze C-C and C -N bond forming reactions employed in the synthesis of active pharmaceutical ingredients (such as Knoevenagel condensation, Henry reaction, Michael addition, and Friedel-Crafts alkylation) are quite rare [63]. In this regard, chemists have looked into more robust and cost-effective catalytic systems that can be adapted to a broad range of reaction conditions, in order to decrease the production costs of synthesis.

2.1. Baeyer–Villiger Reaction

The Baeyer–Villiger (BV) reaction (see Figure 3) is an oxidative pathway bringing to the formation of esters and lactones by oxidation of carbonyl compounds with a peroxide derivative [64]. The reaction takes the name of its two developers, Adolf von Baeyer (previously known for the synthesis of indigo) and his student Victor Villiger, reporting the use of Caro's acid ($KHSO_5$) as a new oxidant for the conversion of cyclic ketones to the corresponding lactones [65]. This versatile protocol was revised in the last century of applications [66]; the interest towards this reaction increased when the work by Fried et al. provided the first definitive evidence of lactone formation in living organisms according to the Baeyer–Villiger pathway [67]. Moreover, the enzymatic B-V oxidation was also explored to facilitate biotransformation of sterically demanding ketones [68]. These evidences opened the way to the search of new oxidants, with major urge in the last 20 years due to the necessity of greener protocols [69,70].

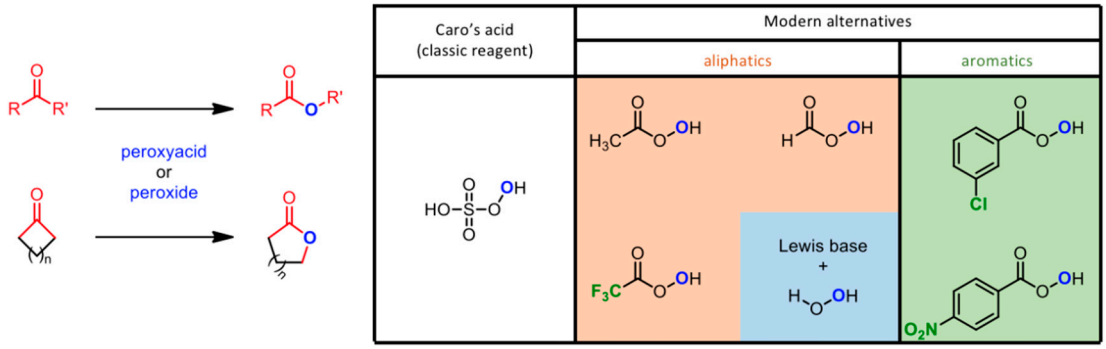

Figure 3. Baeyer-Villiger reaction protocols, and the evolution of commercially available oxidative reagents.

Some interesting papers came out in the middle of the nineties from Kaneda et al., who reported heterogeneous Baeyer-Villiger oxidation of ketones catalyzed by MgAl-CO_3 LDHs using an oxidant combination of molecular oxygen and aldehydes [71]. They also reported higher activity for oxidation of five-membered ring ketones than for that of six-membered ones, with improved yields using mild reaction conditions (40 °C). Successive work reported multi-metallic MgAl LDHs containing Fe ions efficiently oxidizing various cyclic ketones in the same mild conditions, while the exchange of Fe with Cu gave superlative yields with bicyclic ketones [72]. The intuition of the beneficial effects due to the presence of iron in the LDH lattice was also confirmed by Kawabata and coworkers, in the frame of a wider investigation including LDHs with different metal species, such as Fe, Co, Ni, or Cu [73]. An attempt to adapt the procedure to other commercially available oxidants was reported as well [74].

A step towards greener chemistry with no or less harmful chemicals was detailed by Pillai et al., who reported Sn-doped LDHs as efficient and relatively cheap catalysts for BV oxidation reactions, in combination with classic H_2O_2 as oxidizing agent [75]. The mechanism of oxidation was tentatively explained as due to the carbonyl group activation of ketone by the Sn present in the interstitial spaces of LDHs, followed by a subsequent nucleophilic attack by the active peroxide species (peroxycarboximidic acid by reaction of acetonitrile and H_2O_2); the so formed Criegee adduct rearranges to give the corresponding lactone as a final product. Lately, Jiménez-Sanchidrián et al. [76] confirmed the choice of Sn as a primary element to be considered in the design of BV-active LDHs, with reactions running under very mild conditions (atmospheric pressure and a temperature of 70 °C), conversion yields sometimes higher than 80%, and 100% selectivity after 6 h. Among their findings, it is worth noting the evidence that solids containing Zr promoted the decomposition of the hydrogen peroxide and hence adversely influenced the oxidation reaction.

Recent investigations by Olszówka et al. showed that the catalytic performance of MgAl LDHs in cyclohexanone oxidation with H_2O_2 /nitrile system could be significantly improved by the use of Mg-rich catalysts (Mg/Al = 3.69) [77]. Yields up to 50% ε-caprolactone could be achieved in a single-phase reaction medium based on the acetonitrile solvent. The use of acetonitrile rather than the more expensive, more toxic and more difficult to handle benzonitrile, represented a greener and a more economically viable option. Successive structural studies revealed that a lowering of the microcrystalline domains was beneficial for the BV reaction as it improved catalyst's selectivity [78]. This effect was attributed to the observed higher hydrophilicity of less crystalline materials. While it was argued that the enhanced hydrophilicity of poorly crystalline HT samples facilitates the approach and activation of H_2O_2 on surface basic centers, it makes the catalysts more prone to random interactions with the organic substrate, and to its subsequent non-selective transformation [79].

2.2. Knoevenagel Reaction

The Knoevenagel condensation (see Figure 4) is one of the most diffused tools in the hands of organic chemists. Such versatile reaction can be briefly defined as the product of interaction between a

carbonyl compound (aldehyde or ketone) and any compound having an active methylene group. When we say active, we mean that the presence of ancillary electron withdrawing moieties (nitro, cyano, or acyl group) weakens C-H bonds in close proximity. The reaction terminates with a dehydration reaction in which a molecule of water leaves the molecular skeleton. The primary product of a Knoevenagel reaction is usually an α,β-unsaturated ketone [80]. The Knoevenagel condensation is frequently used when building biologically active scaffolds, and it finds application in the synthesis of several biologically-active molecules [81], such as steroids [82].

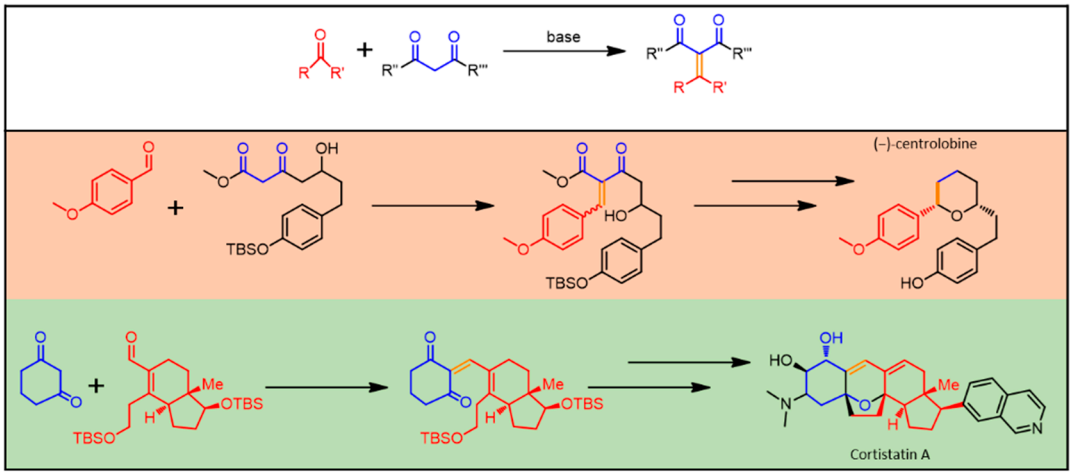

Figure 4. Knoevenagel reaction general scheme. Middle and bottom: examples of some pharmaceutically relevant molecules, whose synthesis involves Knoevenagel condensation. In evidence, the newly formed chemical bond (orange) and the residues belonging to the starting carbonyl (red) and 1,3-diketo (blue) moieties.

An interesting application of LDHs in Knoevenagel reaction goes back to 1999, when Rousselot et al. reported the synthesis of mixed Ga/Al-containing LDHs using different counter-ions (CO_3^{2-}, F^-, and NO^{3-}) and doped with different divalent and trivalent cations (Cu^{2+}, Mg^{2+}, Zn^{2+}, Al^{3+}, Ga^{3+}, Mn^{3+}, and Sc^{3+}) [83]. In their systematic study, they reported on the relative amounts of metallic ions necessary for achieving the best performing material. Besides the structural characterization, the most interesting results regarded the reactivity performance for the Knoevenagel condensation of ethyl cyanoacetate with benzaldehyde. Both calcined and uncalcined materials showed high reactivity; a rehydration process of the calcined samples during the catalytic reaction may explain the similarity. Water, formed together with ethyl cyanocinnamate, would react with the catalysts to give back the original LDH structure.

Fluorinated LDHs (LDH-F) were later developed by Choudary and collaborators in the effort to obtain a more basic (and efficiently) Knoevenagel catalyst [84]. The catalytic clay was prepared starting from a MgAl–NO_3 LDH, which underwent calcination (450 °C) followed by rehydration in presence of KF aqueous solution. The highly polarized basic fluoride ions displayed high catalytic activity both in Knoevenagel condensation (tested the reaction between 2-methoxybenzaldehyde and malononitrile) and 1,4-Michael addition (tested the reaction between acetylacetone and methyl vinyl ketone), under mild liquid phase conditions. The other advantages of LDH-F include easy separation of the catalyst by simple filtration, high atom economy to enable waste minimization, reduced corrosion, and reusability. Such features are certainly appealing for the industrial world converting to greener protocols.

In the general attempt of finding the best combination of experimental parameters, a step forward came from Constantino et al. [85]. In their work, they focused on NiAl-CO_3 LDHs applied to the Knoevenagel reaction involving malononitrile and ethylcyanoacetate, in neat conditions, since the reagents could work as a mixing liquid phase. Mild reaction conditions (60 °C) were sufficient to bring the reaction to completion. Interestingly, during preparation of the heterogeneous catalyst, they

performed a thermal pre-treatment (150 °C per 1 h) claiming that the excellent reaction yields could be due to the anhydrous catalyst that should be able to co-intercalate water molecules generated in the Knoevenagel condensation, and withdraw the reaction equilibrium to the formation of the adduct. Dimethylmalonate, having methylene groups of very low acid strength ($pK_a > 13$) did not give the benzaldehyde adduct, opening the room to chemoselective reactions. Shortly later, the results from Li et al. confirmed the intuition that calcined materials could work in a more profitable way in the context of Knoevenagel protocols [86]. In their study, carbonate-containing LDHs with different combinations of Al^{3+}, In^{3+}, and Mg^{2+} cations were investigated in the condensation of ethyl cyanoacetate with benzaldehyde. The structural characterization pointed out that other relevant parameters should be taken in account, i.e., porosity, surface area, and basicity of the materials, which always exhibited higher values in the case of the more performing calcined materials. Lei et al. moved little further, pointing at the crystallinity of the material [87]. For their MgAl-OH LDHs obtained by calcination/rehydration of MgAl-CO_3 LDH-precursors with high crystallinity, a base-acid catalytic mechanism was proposed to interpret the catalytic behavior. Activated MgAl LDHs synthesized by urea hydrolysis showed a much higher activity in aldol and Knoevenagel reactions than the corresponding material synthesized by the co-precipitation method, suggesting that the presence of acid-base hydroxyl pairs was required, and that catalytic activity was maximized for highly crystalline structures with an ordered array of surface hydroxyl groups. Other groups pursued different approaches towards the improvement of catalytic performance, not related to structural features. Among them, one option was to maximize the basicity of the material, by the introduction of new chemical motifs. In a recent example [88], MgAl LDH-nanosheets were functionalized by grafting aminopropyltriethoxysilane (APTS) onto the clay surface, introducing free amino groups. The prepared MgAl-NH_2 LDH-nanosheets exhibited excellent performance in the Knoevenagel condensation compared to the homogeneous catalyst APTS and the heterogeneous catalysts with Al_2O_3 and SiO_2. These results find reasonable justification in the high surface area of the hybrid nanosheets, and synergistic effects among MgAl LDHs, the grafted -NH_2 groups, and reaction substrates.

Some recent reports tried to conjugate the advantages of heterogeneous catalysis with greener approaches. An example is grafting of LDHs with ionic liquids (ILs). Khan et al. opened the way testing widely described MgAl LDHs (Mg:Al = 3:1), synthesized following published procedures and avoiding pre-treatments, immersed in ILs [89]. Besides the advantageous efficiency of LDH-catalysts and the presence of ILs as a safe and reusable media, they reported also significant alteration in diastereoselectivity in the case of the nitroaldol reaction with nitroethane. In a recent report, Li et al. grafted ILs with different length of their alkyl chains (IL-Cn with n = 4, 8, or 12) onto MgAl-NO_3 LDHs, revealing that the grafting approach helped to adjust the distribution of basic sites, and also induced flexibility to the catalyst, allowing easy accessibility of the active centers by the substrates [90]. Application of LDH-ILs-Cn for Knoevenagel condensation of various aldehydes with ethyl cyanoacetate/malononitrile results in excellent yields, high selectivity, and efficacy in aqueous solution at room temperature, and recyclability as well.

It is here worth mentioning a less conventional approach proposed by Zhou and coworkers, who reported on LDHs developed for the catalysis of two different reactions, which happened in sequence in their case, but that could be easily controlled by the presence/absence of specific chemicals [91]. In more detail, they investigated NiGa LDHs, which could catalyze oxidation reactions and Knoevenagel condensations; in the specific case, alcohols were oxidized to the corresponding carbonyl compound (in the study, benzyl alcohol to benzaldehyde), which reacted in the next step with a partner molecule (benzoylacetonitrile). The introduction of the second partner necessarily ruled the occurrence of the second step, otherwise the simple oxidation would result at the end of the treatment. A good tolerance for the catalyst to various substrates, and excellent recyclability were also reported.

2.3. Michael Addition

The Michael addition reaction (see Figure 5) is generally described as a base-catalyzed addition of a nucleophile, such as an enolate anion, to an activated α,β-unsaturated carbonyl-containing compound, resulting in the formation of a new C-C bond [92]. Since the pioneering work by Arthur Michael [93], this versatile protocol was widely developed for several different fields, ranging from basic research [94] to industrial applications [95].

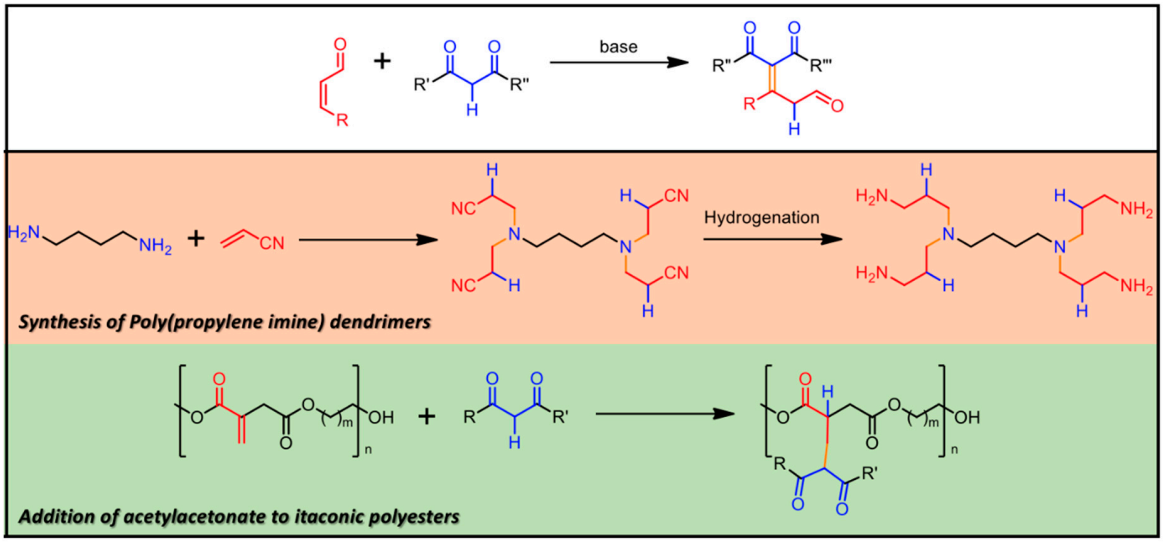

Figure 5. Michael Addition Reaction General Scheme. Middle and bottom: examples of some industrially relevant materials, whose synthesis takes advantage of Michael Addition. In evidence, the newly formed chemical bond (orange) and the residues belonging to the starting carbonyl (red) and 1,3-diketo (blue) moieties.

LDHs play again an interesting role in the recent development of new synthetic routes. A first combination of LDH chemistry and Michael additions came with the work by Choudary et al. [96]. They reported selective 1,4-additions on methyl vinyl ketone, methyl acrylate, simple and substituted chalcones by donors such as nitroalkane, malononitrile, diethylmalonate, cyanoacetamide, and thiols, catalyzed by MgAl LDHs. In their work LDHs, as synthesized or just calcined, showed no relevant activity for the reactions described here, but only the material obtained by decarbonation and subsequent rehydration was an efficient and very selective catalyst. Products of undesirable side reactions resulting from 1,2-addition, polymerization and bis-addition were not observed. Later [97], they discussed the activity of MgAl-OtBu LDHs prepared by incorporating tert-butoxide anion into the interlayer of the clay structure to enhance the basicity of the material. The results were encouraging; reaction yields were reported always to be >85% with mild reaction conditions (room temperature in methanol). Compared with already reported procedures based on non-LDH catalysts, Michael reaction does not entail anymore very long reaction times (in the worst presented case, 2 h vs. 75 h for traditional protocols), high catalyst loading and low yields of the adducts. Waste minimization without any side reactions, use of non-toxic and inexpensive catalysts and recyclability of catalyst are other advantageous features of this procedure. Survey over several reaction parameters (solvent, temperature, and time) was reported by Naciuk et al. [98] who investigated Michael reaction for the synthesis of γ-aminobutyric acid (GABA). Another study on the Michael additions of 2-methylcyclohexane-1,3-dione, 2-acetylcyclopentanone, and 2-acetylcyclohexanone to methyl vinyl ketone interestingly revealed that Mg/Al molar ratio was strongly related to the catalytic performance, pointing out a nonlinear correlation between the Mg content and catalytic activity [99]. This finding would suggest that pure MgO would be more efficient than MgAl LDHs, as they tested and reported, but it causes consecutive reactions of the Michael addition products, which detrimentally reduce product selectivity and yield. Kaneda et al. reported

further insights into the reaction mechanism and the quantification of LDH basic sites [100]. LDH compounds were also used as catalysts in green protocols for Aza-Michael addition. In this regard, in the effort to determine the LDH-catalyst with the highest activity and selectivity, Kantam et al. discussed the reaction between dibutylamine and methyl acrylate (Aza-Michael reaction, due to the amino-group acting as nucleophile) comparing several LDH compounds obtained from calcination and rehydration of different precursors, as well as pure metal oxides [101]. CuAl LDHs proved to be the best candidates, with HT catalyst at room temperature in very good yields. The Cu-Al hydrotalcite showed enhanced activity over the other tested solid catalysts, and it was reused for several cycles with consistent activity and selectivity. One last interesting report concerns LDH-catalysts with anchored L-proline [102]; the catalytic activity was comparable to what reported for other LDHs, but the novelty lay in the asymmetric induction on the Michael addition products. Reaction between β-nitrostyrene and acetone with an inversion in the asymmetric induction was observed when compared to the reaction using pure L-proline catalysis, opening the way to the production of enantiomers using catalysts where the chiral (and expensive) enantiomer is recycled for both the two reactions.

2.4. Transesterification (Biodiesel Production)

The transesterification reaction is one of the universal and well-known tool in the hands of organic chemists. It consists in the exchange of the alkoxy-group of an ester with another one generated by an alcohol; the reaction is reversible, and can be acid-base catalyzed [103]. Besides basic research, it has a never ending number of industrial applications, such as in plastics and polymer technologies [104,105], and biodiesel conversion of biomasses [106].

The importance of basic sites for the catalysis of transesterification induced the scientific community to verify the suitability and performance of LDH-materials. Cantrell et al. reported a deeply detailed investigation over a series of MgAl-CO_3 LDHs [107]. All materials revealed to be effective catalysts for the liquid phase transesterification of glyceryl tributyrate with methanol for biodiesel production. The rate increased steadily with Mg content, with the Mg rich $Mg_{2.93}Al$ catalyst an order of magnitude more active than MgO (comparable results were lately reported by Xie et al. and Zeng et al., in two separate studies using as starting biomass soybean and rape oils, respectively [108,109]). Pure Al_2O_3 (completely inert) was investigated as well for a complete comparison. Their structural investigation resulted in a correlation between reaction rates and intralayer electron density, which could be associated to increased basicity. Some other interesting aspects were revealed by Liu et al. [110]. In their investigation on poultry fat transesterification with methanol, they determined that rehydration of the calcined catalyst before reaction using wet nitrogen decreased catalytic activity, and also, methanol had to be contacted with the catalyst before the reaction took place, otherwise catalyst activity was seriously impaired by strong adsorption of triglycerides on the active sites. Both increased temperature and methanol-to-lipid molar ratio favorably affected the reaction rate. Navajas et al. confirmed these observations about rehydration, and achieved outstanding sunflower oil conversions up to 96% c with 2% w/w of catalyst [111].

Kondawar et al. worked on glycerol transesterification preparing MgAl LDHs, pure or doped with Ca and La [112] (see Figure 6). While the study also interested the simple metal oxides, and CaO showed the highest activity, the formation of soluble calcium glycerate prevented its recovery and recyclability. For this reason, the study justified Ca-doped LDHs as a good compromise between performance and regenerability of the catalyst. Higher activity for Ca-based materials could be traced in the higher basicity obtained for these entries.

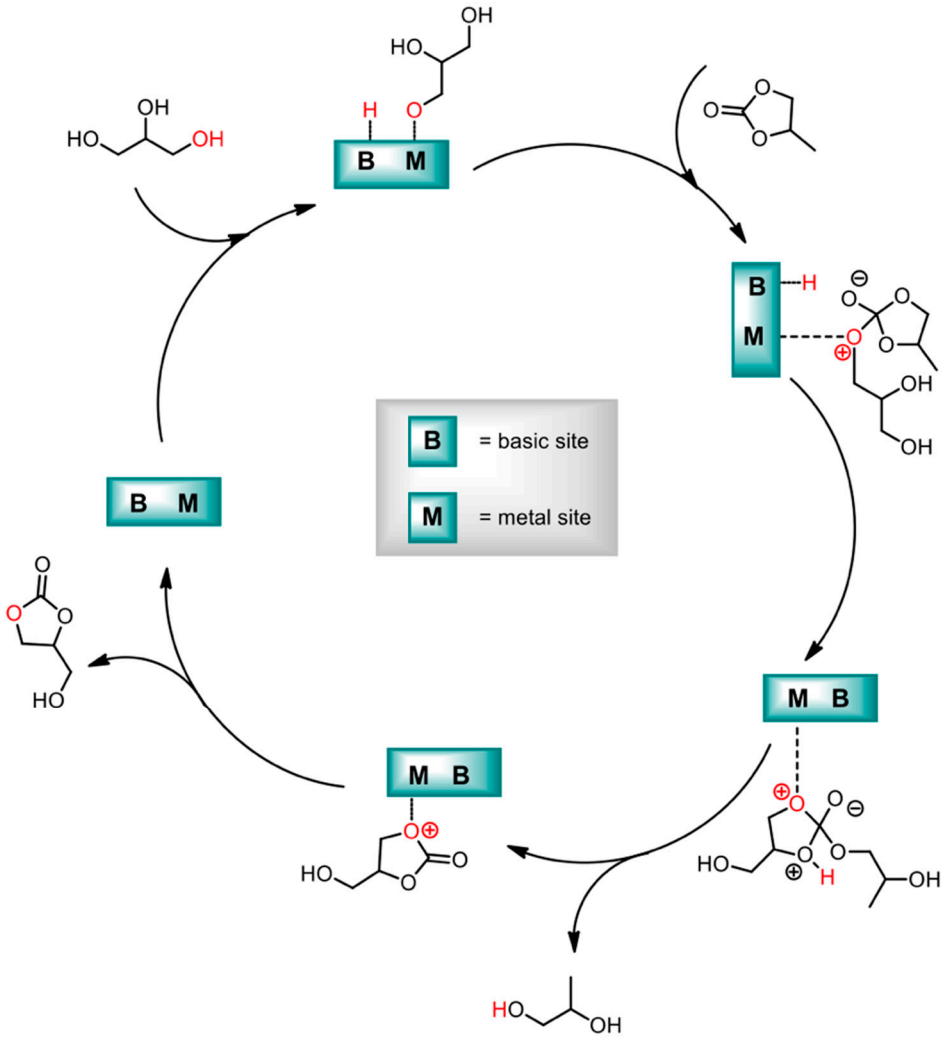

Figure 6. Mechanism of solid-base-catalyzed transesterification of glycerol. Adapted from Ref. [112]. Copyright 2017 American Chemical Society.

Looking for alternative approaches, Yagiz et al. developed MgAl-NO_3 LDHs functionalized with lipase enzymes [113]. The influence of temperature, pH, time and particle sizes was comparatively evaluated on enzyme activity, and the optimum was reached with the immobilization of 13 mg/g of enzyme, working at pH 8.5 and 4 °C. It is reported that the immobilized lipase on HT yielded a lipolytic activity equivalent to 36% of initial activity of lipase, with the relevant advantage of an easy removal of the catalytic hybrid clay at the end of the process and possible recyclability.

3. LDHs Applications in Photocatalysis

In the previous Section, we have discussed in detail some classic organic reactions, and the contribution that LDH-based compounds offer as a catalyst in the development of alternative, greener, and/or more efficient protocols.

A separate section is here dedicated to LDHs in photocatalysis motivated by the following reasons. First, LDHs have been always tested and studied for several applications, e.g., catalysis, with a regular production of literature; in the case of photocatalytic applications, the trend in the publications appears quite anomalous. The first evidences came late in the 80s, with two pioneering reports from the research unit lead by Pinnavaia [114,115]; after that, a negligible number of publications (4 papers in 15 years) was recorded, until the new century coming, with a boom of reports starting from 2008 when two well recognized papers from the team of Vansant received attention from the scientific

community [116,117]. Thereafter, the urge to find answers to the global climate and environmental crisis pushed the accelerator for a new reinterpretation of LDH chemistry. One of the most active researchers in the field of sunlight-driven water splitting, Michael Grätzel, advertised NiFe LDHs as efficient photoactive catalyst electrodes [118]. The volume of publications released in the time window 2016-2019 on photocatalytically active LDHs grew to >150 items. A second reason led us to the creation of a separate section in the present review: although several detailed reviews are available in the recent literature, for example the report from Mohapatra and Parida [119], the number of new available papers calls for a new up-to-date overview.

This section will address three fields of applications, which are hot topics in the recent literature:

i) organic molecules degradation,
ii) water splitting reaction,
iii) CO_2 conversion/reduction,
iv) other examples, which do not belong to the previously mentioned ones.

3.1. Organic Molecules Degradation

Dye molecules are intimately connected with history of humankind, from the prehistoric age to the industrial civilization. Nowadays, although countless applications of dyes, their ubiquitous presence calls for deeper investigations over their implications in environment pollution [120,121]. Many reports closely connect dyes to insurgency of allergic phenomena [122]. It sounds like a paradox, the search for colorants with magnificent properties, for example persistence, ended up in molecules that are difficult to be degraded. The reason why is that chemists pursued different approaches for solving this urgent issue [123–125].

In the last decade LDHs found increasing application in this variegated field, starting from the first report, again from the team of Vansant [126], with increasing attention gained after the publication by Parida and Mohapatra [127], dealing with efficient and cheap ZnFe-CO_3 LDHs. Herein, attention is given to specific LDH compositions focusing on the most recent literature. Zn and Al are recurrent elements in the photocatalytic HT clays formulation [128–135]. Many works report that pristine LDHs can be very efficient without any further treatment, such as calcination, providing decoloration percentage of 90% for solutions of methylene blue (MB) after 1 h irradiation time (better than that of commercial ZnO nanoparticles) [128]. In order to improve the photodegradation performance, additives can be included in the LDH-lattice; cerium doping appeared an interesting option to be considered, as it provided an efficiency 1.5 times higher than pure ZnAl LDH [131] (see Figure 7).

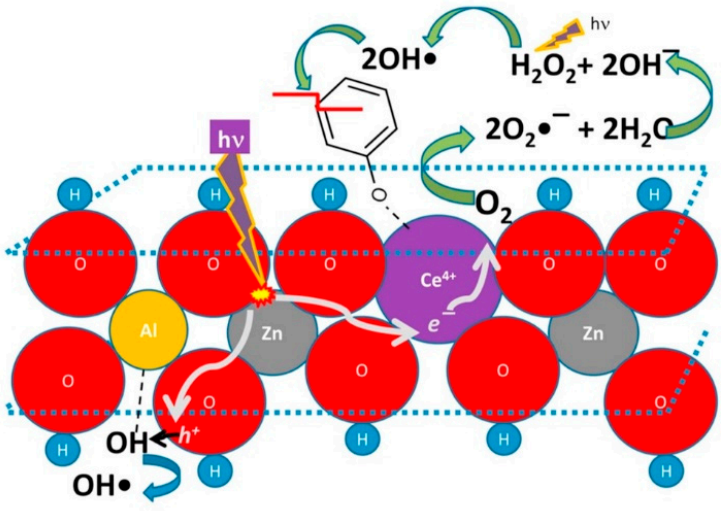

Figure 7. Proposed photocatalytic mechanism for the cerium presence in ZnAl LDH materials and its role as charge separator. Adapted from Reference [131]. Copyright 2016 Elsevier.

A proposed operation mechanism considers Ce^{4+} cations able to: i) Collect e^- photogenerated by the LDH lattice; ii) convert to $*Ce^{3+}$; and iii) transfer the excitation energy (and electron) to an O_2 adsorbed molecule. The so-generated O_2^- radicals can react with water molecules and generate H_2O_2; UV light will break the peroxide and generate highly reactive OH radicals, which are deputed to decompose the organic pollutant (e.g., phenol). In a similar way, lanthanum provided beneficial effect in MB photodegradation operated by doped ZnCr LDHs [130]. However, the integration of TiO_2 in LDHs [134] looks more appealing, since it has the relevant advantage to be a well-known photosensitizer with an extremely low price on the market, making its choice more affordable and convenient for large scale production/application. Another interesting manipulation is the anionic exchange and decoration with Ag_2CO_3, which provided higher selectivity over anionic dyes, as revealed in comparative tests between MB and Red X-3B [129].

In order to find alternative materials where synergic effects could be helpful, Mohamed et al. reported a study over polypyrrole nanofibers coated with ZnFe LDHs [135]. The novel hybrid material was tested for the photocatalytic removal of Safranin dye, or Basic Red 2, a biological stain. The adsorption capability was reported to be about 22% higher than the naked nanofibers, and 31% higher than the pristine ZnFe LDHs. The photocatalytic removal was improved by 42% and 54% higher than the nanofibers and the starting LDHs, respectively.

As a general remark, to be kept in mind throughout the following sections, almost all the specific photocatalytic reactions that we decided to mention in the present work deal with Zn(II)-based LDHs. While the presence of Zn(II) is constant in the reported examples, where Zn seems to be a component of fundamental importance, some works focus their attention over different elemental species. One example is reported by Timár et al. [136]; in their work, the photocatalytic degradation of MB was reported using Mn_2Cr LDHs as photocatalysts. The performance of such LDHs was comparable with commercially available Degussa P25 TiO_2, and remained unaltered over five consecutive runs. Further analyses over materials derived from calcination of the pristine LDHs showed inferior activity; changes in the performance could be traced in the gradual collapse of the layered structure, until no activity could be observed for the photocatalytically inactive double oxide.

3.2. Water Splitting Reaction

LDHs have emerged as highly active photocatalysts for water splitting reaction due to some appealing features. The large surface area and semiconductor characteristics captured the attention of several groups. Some limitations stimulated researchers to exploit modifications of LDH-based photocatalysts. Among them, Fu et al. reported on the doping procedure of ZnCr LDHs with terbium cations, demonstrating an improved photocatalytic performance [137]. Photoluminescence and photoelectrochemistry measurements on the ZnCrTb LDH samples revealed a more efficient charge carrier separation and higher injection efficiency, compared to the pristine non-doped ZnCr LDHs. Optimal performances were observed for a specific doping level (0.5%), with a 2-fold increase in photocatalytic O_2 production efficiency. Oxygen generation through photocatalytic water splitting under visible light irradiation was studied by Gomes Silva et al., who investigated a series of ZnTi, ZnCe, and ZnCr LDHs at different Zn-to-metal atomic ratio (from 4:2 to 4:0.25) [138]. ZnCr LDHs proved once again to be the best matching case, with an atomic ratio of 4:2. The authors focused on the apparent quantum yields for oxygen generation, with values well comparable with previous results by Fu et al. It is worthwhile to point out that these quantum yields (60.9% and 12.2% at 410 nm and 570 nm, respectively) were among the highest values ever determined with visible light for solid materials in the absence of a light harvesting dye. Interestingly, in a field of rapid growth, it is appreciable that different research groups arrived to the confirmation of similar findings, further supporting and consolidating the trend in photocatalytic exploitation of LDHs.

Lee and coworkers followed a different approach to the improvement of photocatalytic performances, with specific focus over the other half-reaction, bringing the evolution of H_2 [139]. In their case, the material consisted of a combination of graphitic carbon nitride (g-C_3N_4), which acted

as a support for ZnCr LDH nanocrystals. Structural characterization and investigation of surface area confirmed the localization of the nanocrystals in the mesopores of the graphene-like lattice; an efficient electronic coupling between both the two components of the hybrid material gave rise to the observed enhanced visible light absorptivity and suppression of electron−hole recombination.

In two different reports [140,141], photoanodes were successfully prepared by the integration of bismuth vanadate $BiVO_4$ with Co-based LDHs (see Figure 8). The design presented by Vo and collaborators was more complex, bringing to the preparation of a CoMnZn trimetallic anionic clay, but several details are herein discussed. The evidences suggested synergistic effect of the three-metal composition towards the enhanced photoelectrochemical performance. Surface modification of photoanodes with trimetallic hydroxides greatly improved the migration of holes from bismuth vanadate to LDH, facilitating fast separation and transport of holes, thus retarding the recombination of photogenerated charges.

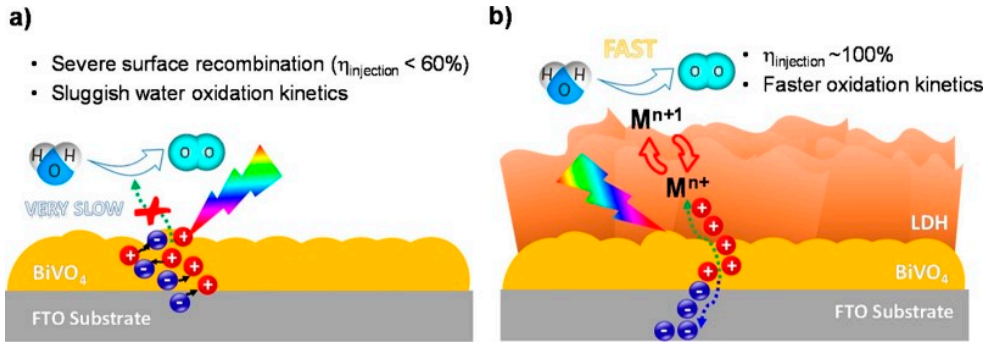

Figure 8. Schematic representation of charge carrier dynamics in water oxidation on BVO (**a**) and BVO/CMZ-LDH (**b**) photoelectrodes. Adapted from Reference [141]. Copyright 2019 Elsevier.

3.3. CO_2 Conversion/ Reduction

Photocatalytic conversion of CO_2 into alcohols is a chemical pathway widely pursued in order to answer two relevant issues. From one side, to find application to an inert molecule which is the last step of carbon oxidative chain, and a dangerous greenhouse gas as well. From the other side, it is a way to produce liquid fuels in an environmentally compatible manner and in a less energy demanding way. Several different approaches and materials were tested [142–144], and LDHs resulted to be an intriguing option also in this case. Some interesting achievements concerned MgAl LDHs, which are the simplest, most common, and deeply studied HT compounds. Their high CO_2 adsorption performance, even at room temperature, was already reported [145]. Among the latest reports, Flores-Flores et al. focused on the development of a microwave-assisted protocol for catalytically active LDHs [146]. As the authors claimed, MW-irradiation was necessary to produce samples with high crystallinity, which had a strong impact over methanol production rate. During the photocatalytic experiments, under halogen lamp irradiation, MgAl LDHs showed higher selectivity for CH_3OH production in liquid phase than in gas phase, due to a more negative flat band potential to carry out the CO_2 reduction. Iguchi et al. played with the composition of MgAl LDHs, introducing fluorine species in the lattice (e.g., AlF_6^{3-} anions) [147]. In their reports, they observed that the reduction cascade led to the selective production of CO under UV-light irradiation. A highly selective compound for CO_2 photoreduction into methanol employed ZnCuGa-CO_3 LDHs [148]. In the paper, the photocatalytic material was required to be heated at 150 °C in vacuum in order to reduce the content of interlayer water by 31%; after this stage, if LDHs never got in contact with air prior to the photoreduction tests, methanol production selectivity was verified to be >97% in all the studied cases.

A change in the divalent cation (Ni instead of Mg) was demonstrated to modify the outcome of the catalysis; e.g., the resulting NiAl LDHs showed 80% selectivity towards CO among the reduction products after 20 h of UV light irradiation. The substitution of metal cation came from another broad investigation over 16 different kinds of transition metal containing $M^{2+}M^{3+}$ LDHs (M^{2+} = Co, Ni, Cu,

Zn; M^{3+} = V, Cr, Mn, Fe) applied to the photocatalytic conversion of CO_2 to CO in an aqueous solution of NaCl [149]. A *summa* of these results can be finally seen in the investigation reported by Tokudome et al., where NiAl LDHs were tested as nanocrystals [150]; the remarkable rate of photocatalytic CO_2 reduction by the nano LDH catalyst was reported to be almost one order of magnitude (7 times) higher than that measured by means of LDH catalyst prepared through conventional methods. It looks like the research unit made a step backward, ignoring the best performances offered by NiV LDHs, which were supposed to benefit from the implementation of nanoforms. It can be argued, however, that vanadium is more expensive and exotic than well established (and cheap) aluminum.

Crystallinity is a recurrent keyword in the work of Zhao et al. [151]. In their work, they compared the synthetic protocols for MgAlTi LDHs (co-precipitation, co-precipitation + hydrothermal, and co-precipitation + calcination + reconstruction). Crystalline TiO_2 domains were present in the LDHs obtained by hydrothermal or reconstruction processes. The material hydrothermally treated at 150-200°C demonstrated the highest CO production due to a well-balanced TiO_2 crystallinity and specific surface area. Compared with commercial TiO_2-P25 nanoparticles, MgAlTi LDHs demonstrated 2 to 4 times higher catalytic activity in CO_2 photoreduction to CO.

Another example calls back what was already described for LDH application in water splitting reaction. The work from Tonda et al. exploited the possibility to take advantage of a two-component hybrid combining *g*-C_3N_4 with LDHs [152] (see Figure 9). In the present case, a detailed characterization and description of the photocatalytic mechanism in the *g*-C_3N_4/NiAl-LDH heterojunction culminated in the observation of a CO production rate 5 times higher than that of pure *g*-C_3N_4, and 9 times higher than what was revealed for pure NiAl LDHs.

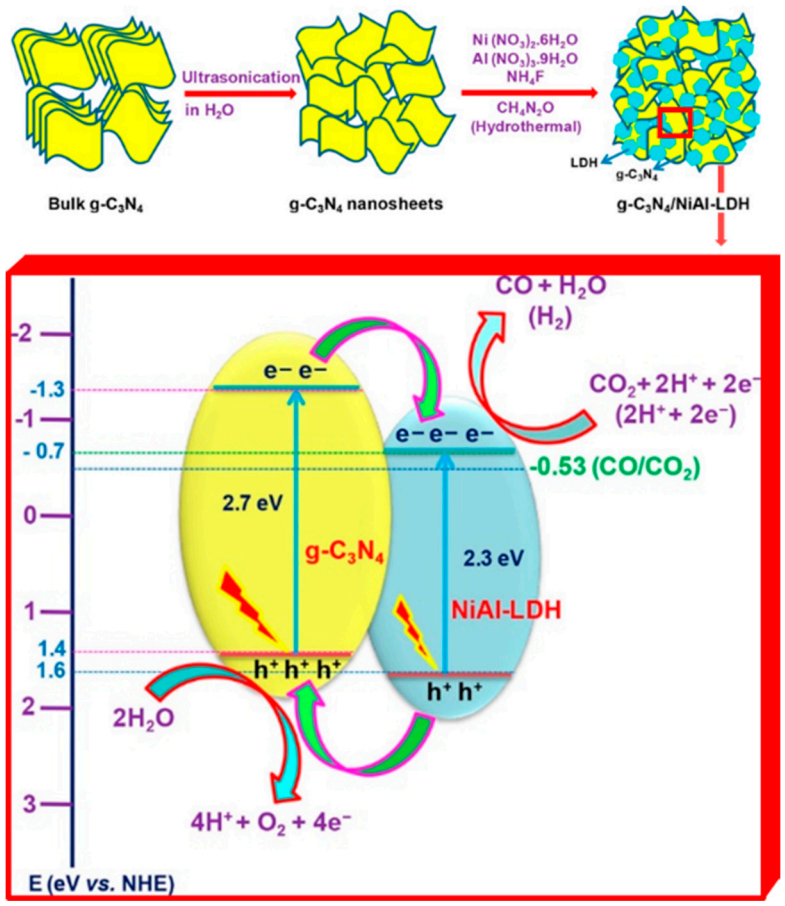

Figure 9. Top. Schematic illustration of the synthesis process of *g*-C_3N_4/NiAl-LDH hybrid heterojunctions. Bottom. Proposed mechanism for CO_2 photoreduction in the *g*-C_3N_4/NiAl-LDH heterojunctions. Adapted from Reference [152]. Copyright 2018 American Chemical Society.

3.4. Others

In this section, a couple of interesting papers focusing on other relevant topics are discussed. In the previous Section, several words have been spent over transesterification as an important route to produce biodiesel. Again, LDH materials are used, as well, in photocatalytic applications close to the petroleum chemistry, as Gao et al. reported [153] (see Figure 10). LDHs were employed in the mitigation of polluting emissions of diesel oil, mostly related to the high concentration of sulphur-containing hydrocarbons [154]. Their LaZnAl-MoO_4 LDHs were reported to promote desulfurization of diesel oil under UV irradiation, favoring the oxidation of dibenzothiophene (DBT) to the corresponding sulphone. The conversion rate, based on the quantity of sulfone that remained adsorbed to the LDH surface, was determined as being up to 84% in 1 h.

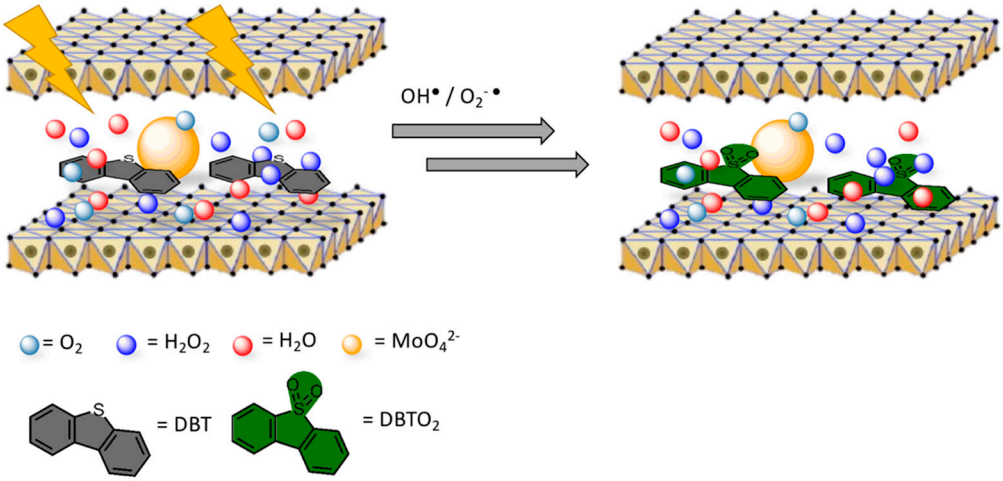

Figure 10. Catalytic oxidation of dibenzothiophene (DBT) on $LaZnAl_3$-MoO_4 LDH-catalyst. Adapted from Reference [153]. Copyright 2018 Taylor and Francis.

To justify their evidences, they claimed that MoO_4^{2-} anions increased the interlayer space promoting the adsorption of dibenzothiophene (DBT), which is one of the most relevant sources of sulphur in the oil. Synergistically, MoO_4^{2-} acted as the active sites for the oxidation of DBT, resulting in the high desulfurization efficiency. These statements were justified by comparing the molibdate LDH-photocatalyst with an equivalent one with carbonate anions, which showed inferior desulfurization performance. The presence of La^{3+} cations was mandatory, since they brought more positive charge to the brucite-like sheets, leading to an improved adsorption of molibdates on the surface of the layers.

Photocatalytic LDHs found application in the improvement of another fundamental process: N_2 fixation. The reaction consists in the reduction of gaseous N_2 to ammonia, NH_3; it is an essential mechanism for the production of nitrogen containing biological molecules [155], as well as industry relevant products, such as fertilizers [156]. The Haber-Bosch process [157], one of the most important processes of human history, produces ammonia under extreme conditions cycle (400–500 °C, 200–250 bar), leaving room for improvements and discovery of more convenient alternatives. Zhao et al. reported the photocatalytic activity of ultrathin LDH nanosheets (NSs) made with different combinations of di- and trivalent metal cations (M^{2+} = Mg, Zn, Ni, Cu; M^{3+} = Al, Cr) [158]. The most promising samples were the CuCr-LDH NSs; photocatalytic reduction of N_2 to NH_3 was observed in water at 25 °C under visible-light irradiation, with quantum yield of about 0.44% at 380 nm and 0.10% at 500 nm. Monochromatic light of wavelength 500 nm afforded a NH_3 evolution rate of about 7.1 μmol L^{-1}, which was a great achievement considering that the authors were far away from the UV and significantly closer to the maximum of solar emission spectrum. The photocatalytic activity was attributed to the

distorted structure in the LDH NSs, which is supposed to enhance N_2 chemisorption and to promote NH_3 formation.

4. LDH Applications in Biosensors

LDHs have been largely employed as efficient biosensors, owing to their excellent biocatalytic properties and to the possibility of producing hybrid materials with enzymes. Starting from the first example of urea biosensors based on the immobilization of urease into oppositely charged clays [159], most of the research in the field of LDH-based biosensors was devoted to the fabrication of oxidoreductase enzyme/LDH amperometric biosensors, where typically employed enzymes were transketolase, acetylcholinesterase, horseradish peroxidase, and glucose oxidase [160]. The researchers also showed the possibility to prepare hybrid LDHs containing redox active molecules as enzyme immobilization matrices, such as anthraquinone sulfonate, ferrocene, and 2,2′-azinobis 3-ethylbenzothiazoline-6-sulphonate.

In general, the class of enzyme-based biosensors is featured with high costs and low stability, being their response potentially affected by factors such as temperature, pH, and ionic strength [161,162]. For these reasons, recent research efforts were focused on the fabrication of enzyme-free biosensors mostly based on the functionalization of electrodes with functional nanomaterials, benefiting from low costs, rapid response, high sensitivity [163], and from the possibility to enhancing electrode activity providing much more accessible exposed active sites as well as to provide convenient ion/electron transport channels for electrochemical detection of analyte molecules. In this scenario, LDHs have been explored as convenient materials for the fabrication of enzyme-less glucose biosensors. As a remarkable example, Cui et al. [164] reported on the fabrication of a bifunctional non-enzymatic flexible glucose microsensor based on CoFe LDHs by directly growing a CoFe layered double hydroxide nanosheet array (LDH-NSA) on a Ni wire. The LDH system showed high sensitivity and high selectivity in electrochemical and colorimetric detection of glucose, with linear ranges from 10 to 1000 mM and from 1 to 20 mM, and detection limits of 0.27 μM and 0.51 μM, respectively. The electrocatalytic glucose oxidation mechanism of CoFe LDH was tentatively explained by the authors, as follows:

$$\text{LDH-Co(II)} + OH^- \rightarrow \text{LDH}(OH^-)\text{Co(III)} + e^-$$
$$\text{LDH}(OH^-)\text{Co(III)} + \text{glucose} \rightarrow \text{LDH-Co(II)} + \text{gluconolactone}$$

As further examples, Ai et al. modified glassy carbon electrodes with a NiAl LDH composite with chitosan, obtaining a good linear range (0.01–10 mM) for glucose detection [165]. Li et al. employed NiAl LDHs onto titanium electrodes, obtaining a detection limit of 5 μM and a linear range up to 10.0 mM [166]. More recently, the preparation of a glassy carbon electrode modified with a composite material based on gold nanoparticles decorated with NiAl LDHs and single-walled carbon nanotubes permitted to obtain a wide linear range from 10 μM to 6.1 mM [167]. The authors ascribed the good detection performances to the combined effects of enhanced electrical conductivity deriving from 3D network formed by carbon nanotubes, good accessibility to active reaction sites from NiAl LDH and more electron transfer passages provided by Au nanoparticles. Besides glucose, non-enzymatic LDHs-based sensors have also found applications in the detection of drugs, such as Terazosin hydrochloride, an Alpha-adrenergic Blocking Agent, by means of MgAl LDHs [168], or for the detection of nitrite ions from solution by NiFe LDHs fabricated onto carbon cloth substrates [169].

As another pivotal example, Asif et al. demonstrated the easy fabrication of hybrid LDH nanosheets with layers of reduced graphene oxide for electrochemical simultaneous determination of dopamine, uric acid and ascorbic acid [170]. They produced such 2D composite material by following a coprecipitation route in which the ZnNiAl LDH and GO precursors were added dropwise to a formamide solution with continuous stirring. In another synthesis procedure, they directly mixed ZnNiAl LDH and GO supernatant solutions and added hydrazine in order to obtain reduced GO. The latter synthesis approach allowed to self-assemble a periodic superlattice compound by integrating positively charged semiconductive sheets of a ZnNiAl LDH and negatively charged layers of reduced

graphene oxide. By operating at typical working potentials of −0.10 V, +0.13 V, and +0.27 V vs. saturated calomel electrode, the obtained lower detection limits for ascorbic acid, dopamine, and uric acid were 13.5 nM, 0.1 nM, and 0.9 nM, respectively. The authors also showed the possibility to track the dopamine released from human neuronal functioning neuroblastoma cell line SH-SY-5Y after being stimulated by highly K^+ buffer.

Along with electrochemical sensors, many efforts focused on the preparation of LDH-based sensors with fluorescence readout. Recently, Liu et al. demonstrated a fluorometric displacement assay for measuring the concentration of adenosine triphosphate (ATP) using layered cobalt(II) double hydroxide nanosheets [171]. In particular, they used a dye-labeled oligonucleotide adsorbed on the LDHs. The adsorption led to the complete and fast quenching of the green fluorescence of the label. In presence of ATP in the solution phase, the DNA oligonucleotide was rapidly detached from the LDH because of the stronger affinity of ATP for LDH, finally leading to the restoration of the green fluorescence signal. This remarkable effect was used by the authors to produce an assay showing a linear response in the 0.5–100 μM ATP concentration range and a 0.23 μM lower detection limit, allowing for the determination of ATP in spiked serum samples. In a similar approach, Abdolmohammad-Zadeh et al. showed a fluorescent sensor based on nanostructured MgAl LDH intercalated with salicylic acid (SA) for sensing the ferric ions in solution [172]. The calibration graph was linear in the concentration range of 0.07–100 μmol/L, along with a detection limit of 26 nmol/L. The authors demonstrated the intercalation of salicylic acid into the layers of the host Mg-Al LDH matrix by showing an increased interlayer spacing as measured by XRD analysis. The fluorescence intensity of salicylic acid was increased by its intercalation into LDHs, given the effect of confinement, which reduced the interaction between salicylic acid and the solvent. In presence of Fe^{3+} ions, the fluorescence signal of MgAl LDHs intercalated with SA decreased with increasing of Fe^{3+} ions concentration because of the formation of a stable complex with salicylic acid.

Among optical based techniques, chemiluminescence is also a powerful approach for biomolecular detection given its high sensitivity and low cost in comparison to fluorescence [173]. Many reports have shown the possibility to employ LDHs for the realization of chemiluminescent glucose sensors. For instance, Wang et al. demonstrated that MgAl LDHs can be supporting materials for immobilizing luminol reagent, by triggering luminol chemiluminescence in a moderately acid pH (5.8). In the presence of horseradish peroxidase, the luminol-LDH hybrid was able to produce chemiluminescence signal to glucose in the range of 0.005–1.0 mM, along with a detection limit for glucose equal to 0.1 μM [174]. In another paper, Pourfaraj et al. demonstrated that CoNi LDHs exhibit catalytic activities towards the luminol-H_2O_2 reaction. Under optimum conditions, the chemiluminescence intensity was linear in the range 0.1–12μM of H_2O_2 concentrations along with a detection limit (S/N=3) of 0.05 μM [175]. More recently, Pan et al. demonstrated the possibility to use the LDH–luminol–H_2O_2 system-based chemiluminescence platform for sensing carminic acid, a colorant used in food additives [176]. The detection principle consists of two steps: First, LDH adsorbs carminic acid onto the surface, then the carminic acid quenches the chemiluminescence of the LDH–luminol–H_2O_2 system by resonance energy transfer, reduction of reactive oxygen species, and occupation of the brucite-like layers. The authors demonstrate the possibility to obtain a linear response to the analyte in the concentration range from 0.5 to 10 μM, along with a limit of detection equal to 0.03 μM.

Telomeric DNA could also be a target analyte as recently shown by Haarone et al. [177], who produced a MgAl LDHs intercalated with DAPI (4′,6-diamidino-2-phenylindole), which is a fluorescent molecule that strongly binds to adenine–thymine rich regions in DNA sequences. DAPI could assemble into the LDH nanosheets by blending with single strand DNA via the co-assembly method (see Figure 11). The DAPI containing LDH was able to detect long single strand DNA/telomere sequences simply by changing the single strand DNA sequence. The authors demonstrated a dynamic range within the 3–20 μg/mL range along with a detection limit of 20 μg/mL.

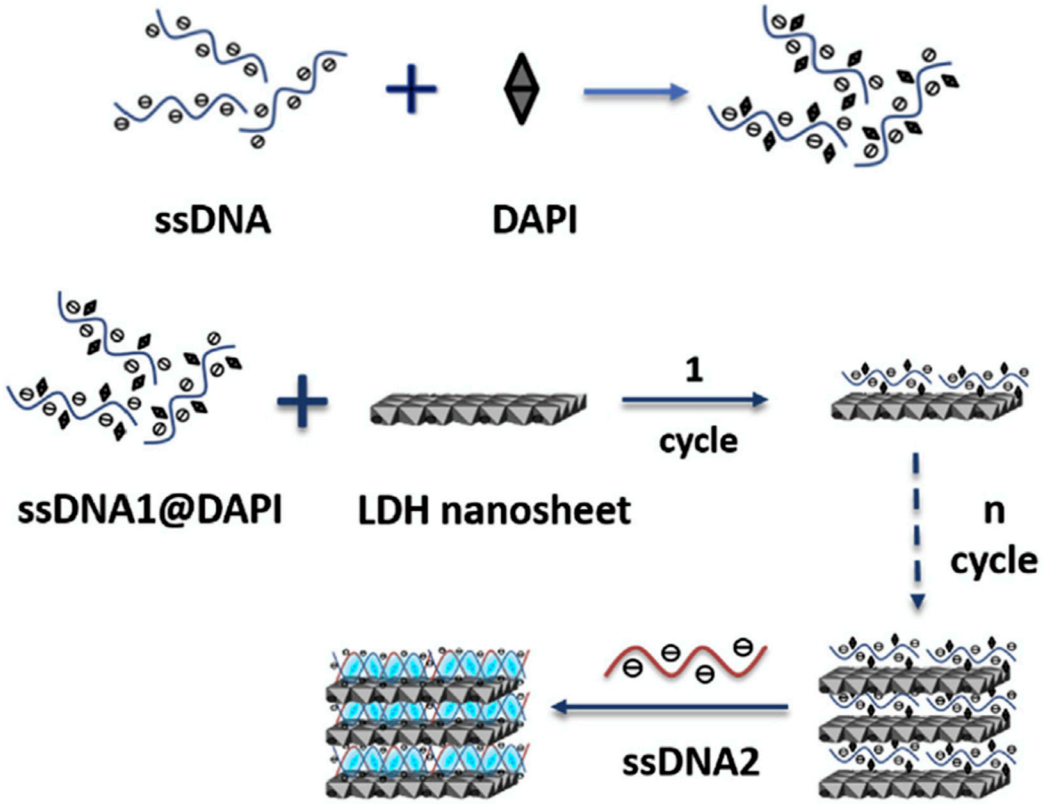

Figure 11. Scheme of the assembly of ssDNA blending into DAPI/LDH ultrathin nanosheets. Figure readapted from Ref. [177], with permission from Elsevier.

Finally, LDHs could be applied for guanine detection by means of silver nanoclusters (AgNCs) stabilized by nuclear fast red (NFR) sodium salt on Mg_2Al LDH nanosheets [178]. Due to the confinement effects in 2D layered LDH nanosheets, the fluorescence intensity and photostability of the AgNCs-NFR/LDH compound were significantly improved if compared with those of the AgNCs-NFR based solution. By introducing Cu^{2+} ions as a modulator, AgNCs-NFR/LDHs were successfully applied for determining guanine in the concentration range of 10 μM–100 μM, along with a detection limit equal to 1.85 μM. Recently, dopamine biosensors for real time detection of dopamine (detection limit down to 2 nM) from live cells (human neuronal functioning neuroblastoma cell line SH-SY 5Y) were realized in the form of composite materials produced by exfoliated charged nanosheets of LDHs and graphene [179]. Similarly, carbon nanotubes loaded onto a CuMn LDH nanohybrid allowed for a high-sensitivity electrochemical detection of H_2S from live A375 cells (detection limit equal to 0.3 nM) [180].

5. LDHs Applications in Nucleic Acids (DNA, RNA) Delivery

Besides sensing molecules and nucleic acids in biological samples, LDHs can find important applications in life sciences given their ability to deliver biomolecules to biological systems. LDHs are efficient drug delivery systems, possess good biocompatibility, high drug-loading density, high drug-transportation efficiency, low toxicity to target cells, or organs, offering excellent protection to loaded molecules from undesired enzymatic degradation [160,181]. DNA is the carrier of the genetic information in living cells. The structure of DNA consists in two single strands of DNA, which can bind together by hydrogen bonding between complementary pairing bases (adenine to thymine and guanine to cytosine), thus forming the well-known DNA double helix structure. DNA delivery to cells represents one of the most investigated applications for the biological sciences. In this regard, the successful DNA delivery to cells strictly requires that the foreign DNA material must remain stable

within the host cell by fusing into its genome or retaining the ability to integrate intracellularly replicate. This requires foreign DNA to be delivered by a suitable vector, which has the capability to enter the host cell and accurately deliver the DNA molecule to the cell's genome, being the vectors employed for gene delivery sorted into recombinant viruses and synthetic vectors. Similar to DNA, RNA is self-assembled as a chain of nucleotides, with the only difference that uracil is used instead of thymine. RNA has many important roles in biological organisms, such as conveying the genetic information and directing protein synthesis. In the last ten years, RNA molecules were being processed via the RNA interference (RNAi) pathway, which consists in silencing the expression of genes with complementary nucleotide sequences by degrading the mRNA after transcription from DNA, ultimately preventing translation. In this regard, the small interfering RNA (or silencing RNA, siRNA) therapy is hampered by the barriers for siRNA bioavailability to enter into cells cytoplasm and exert their gene silencing activity. In this scenario, LDHs have been demonstrated as an ideal synthetic vector for both DNA and RNA molecules, due to a well-elucidated adsorption mechanism, taking into account that the phosphate backbone of the DNA polymer coordinates with the metal cations of the LDH lattice via the ligand-exchange process [182,183].

The formation of LDH-DNA hybrids for DNA delivery can be obtained either through the incorporation of small DNA molecules and antisense oligonucleotides into the LDH matrix by a simple ion-exchange reaction [184], or by a more general coprecipitation route involving the in situ formation of LDH layers of various ionic compositions around intercalated DNA [185]. In particular, the feasibility of the latter approach was demonstrated by Desigaux et al. [185] that demonstrated the intercalation of DNA into the LDH matrix by the net increase of the interlayer distance, from ~0.77 nm for all nitrate parent LDHs to ~2.11 nm, ~1.80 nm, and ~1.96 nm for DNA molecules complexed with Mg_2Al, Mg_2Fe, and Mg_2Ga, respectively (see Figure 12). Choy et al. were the first that showed the possibility to intercalate c-myc antisense oligonucleotide (As-myc) into MgAl LDH nanoparticles by anion exchange [186].

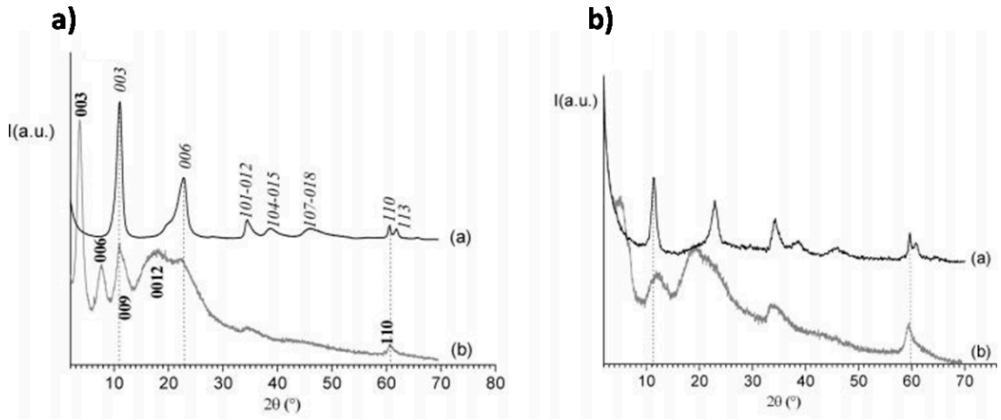

Figure 12. Powder X-ray diffraction patterns in the 2θ range 2°–70° of LDH/DNA Hybrids. (**a**) Mg_2Al/NO_3 (spectrum a) and Mg_2Al/DNA (spectrum b). (**b**) Mg_2Fe/NO_3 (spectrum a) and Mg_2Fe/DNA (spectrum b). Reprinted with permission from Ref. [185]. Copyright (2006) American Chemical Society.

The results from cellular internalization experiments demonstrated a strong inhibition of the proliferation of HL-60 cancer cells exposed to As-myc–LDH hybrids, reaching 65% growth inhibition compared with untreated cells. In a more recent report, ZnAl LDH nanoparticles were loaded with the plasmid pCEP4 to permit the expression of the Cdk9 gene in C2C12 myoblasts cells, as confirmed by PCR and Western blotting results [187]. They were also loaded with valproate and methyldopa drugs, allowing for sustained pH-triggered drug delivery. With the aim to combine dissipative molecular-dynamics simulations and experimental work, Li et al. [188] demonstrated that delaminated LDH-DNA bioconjugates can penetrate the membrane walls of plant cells (BY-2 cells). The authors

delaminated the LDH nanoparticles by intercalating lactate into the layers of LDH nanoparticles. They also demonstrated that only the DNA-LDH-DNA sandwich complex was efficiently taken by the cells, whereas LDH-DNA-LDH sandwich complex and the DNA-LDH complex were not compatible for intracellular delivery, mainly due to the fact that the hydrophobic sequences of DNA provided a driving force for penetration. For example, the DNA-LDH-DNA sandwich complex was gradually internalized into the membrane to minimize exposure of the DNA hydrophobic sequences in the hydrophilic solvent.

Along with the above reported methods, DNA oligonucleotides can be also immobilized by silanization of LDHs in aqueous suspension as demonstrated by Ádok-Sipiczki et al. [189]. In particular, the 3-aminopropyltriethoxysilane (APTES) was employed as linker. APTES covalently attached to the MgAl LDHs. In turn, the amino group of the APTES linker reacted with the activated 5′ carboxylic functional group of the nucleic acid strand, for the activation of which 1-ethyl-3-(3-dimethylaminopropyl) carbodiimide hydrochloride salt (EDC) and N-hydroxysuccinimide (NHS) were used. The EDC reacts with the carboxylic group of the nucleic acid to form the O-acylisourea mixed anhydride. The addition of a selected nucleophile such as NHS, which reacts faster than the competing acyl transfer, generates an intermediate compound being active enough to couple with the amino group, finally also preventing any possible side reactions. The authors conclude that the covalent linkage of the nucleic acids confers to this model nanoparticulate system promising properties and potential for applications as therapeutic agents, since the DNA could be taken into the cells allowing for intracellular delivery.

In a similar way to DNA, also RNA complexed with LDHs nanoparticles can be delivered to cells, being the application of siRNA the main driving force for developing this type of molecular delivery. For instance, Wong et al. [190] reported the delivery of siRNA to primary neuron cells resulting in the silencing of gene expression. This possibility has important applications for potential diseases such as the treatment of neurodegenerative conditions (e.g., Huntington's disease). Interestingly, authors found that it was possible to produce Mg_2Al LDHs for simultaneously deliver anticancer drug 5-fluorouracil (5-FU) and Cell Death siRNA for effective cancer treatment, by loading the siRNA on the surface of LDH nanoparticles and the 5-FU into interlayer spacing [191]. Compared to treatment with only CD-siRNA or 5-FU, the combination of the two different molecular systems led to an enhanced cytotoxicity to three cancer cell lines, i.e. MCF-7, U2OS, and HCT-116. This interesting synergic effect was ascribed to a coordinated mitochondrial damage process. In another interesting approach, Park et al. [192] showed the possibility to obtain an efficient in vivo and in vitro delivery system for Survivin siRNA assembled with either passive MgAl LDHs, with a particle size of 100 nm, or active LDHs conjugated with a cancer overexpressing receptor targeting ligand, folic acid (LDHFA). These routes allowed targeting the tumor by either EPR-based clathrin-mediated or folate receptor-mediated endocytosis. The authors also showed the ability to induce potent gene silencing at mRNA and protein levels in vitro, and achieved a 3.0-fold higher suppression of tumor volume than LDH/Survivin in an in vivo tumor mouse model. Another interesting example of RNA intercalation in LDHs was provided by Acharya et al. for potential application in neurodegenerative diseases [193]. They employed short hairpin RNA (shRNA) intercalated in MgAl LDH nanoparticles at the mass ratio of (1:75), leading to the formation of shRNA-plasmid-LDH nanoconjugates, with an average size of 40–60 nm, which were efficiently transfected into mammalian neuroblastoma cells (SH-SY5Y), observing a maximum internalization of ~26% at 24 h. This, in turn, led to a significant downregulation of the protein alpha TNF, demonstrating the efficient functionality of the delivered shRNA.

In the case of CaAl LDH nanoparticles, the pH at which these nanomaterials are prepared can affect the efficiency of RNA uptake [194] (see Figure 13). Rahaman et al. showed that the involvement of carbonate ion as impurity was critical during the preparation of CaAl LDHs (see Figure 13). The authors prepared CaAl LDHs at two different pHs, i.e., pH 8.5 vs. pH 12.5, finding that at the higher pH, more carbonate ions were intercalated into the CaAl LDH structure, leading to lower intercalated RNA, as demonstrated by FTIR and XRD characterizations. In particular, after intercalation of shRNA

the *d* spacing of the basal plane (0 0 2) increased from 8.61 Å in the phase pure CaAl LDH to 20.30 Å in shRNA sample. Interestingly, these data were nicely correlated with cellular uptake using colon cancer cell line (HCT 116), since LDHs prepared at pH 8.5 led to a significantly higher uptake (9.34%) in comparison to LDHs prepared at pH 12.5 (3.54%).

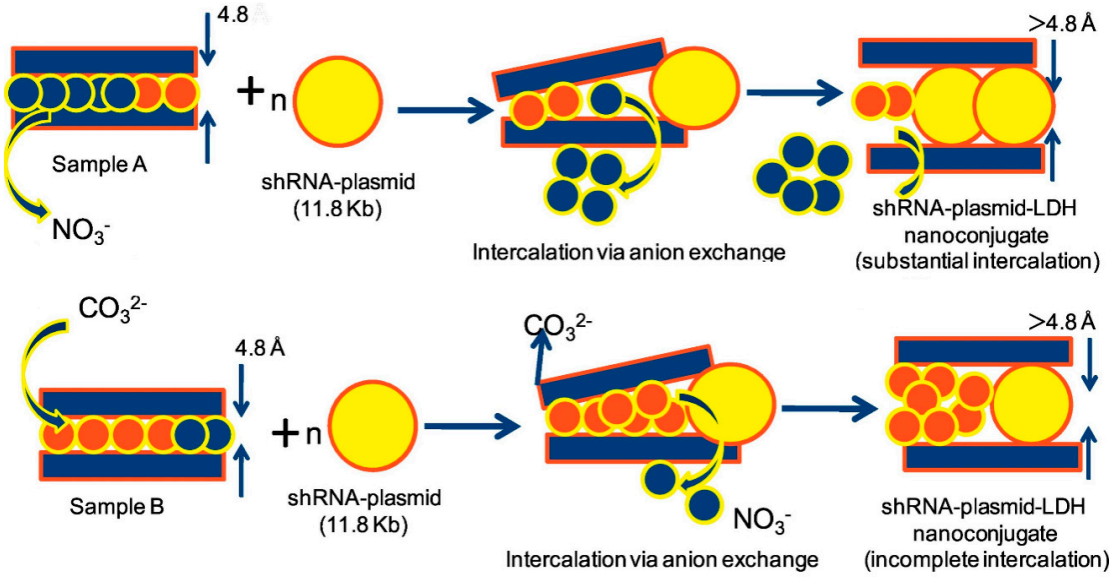

Figure 13. Schematic representation of the mechanism of intercalation of anionic shRNA-plasmid, in presence of NO_3^-/CO_3^{2-}, in cationic layers of samples A (precipitated at pH 8.5) and B (precipitated at pH 12.5). Reprinted from Ref. [194], Copyright (2019), with permission from Elsevier.

In more recent reports, the researchers strived to the aim of improving the efficacy of LDH delivery of RNA in comparison with other nanomaterials. For example, Li et al. [195] demonstrated that siRNA could be more efficiently delivered to osteosarcoma (U2OS) cells by mannose-conjugated SiO_2 coated LDH nanocomposites (Man-SiO2@LDH) compared to unmodified LDH NPs. The enhanced uptake was attributed to the active mannose-receptor interaction-mediated endocytosis, considering also the specific strong binding affinity towards lectin that is expressed on the cancer cell membrane.

Wu et al. [196] compared LDHs and lipid-coated calcium phosphate nanoparticles (LCPs) as effective vectors for siRNA delivery into suspended T lymphocytes (EL4) for silencing the target PD-1 gene. They found that LCPs showed a higher cellular uptake and higher PD-1 gene silence efficiency in mouse T cell line EL4 (about 70%) in comparison to LDHs (40%). They ascribed this difference to the smaller size of the LCPs with respect to LDHs (50 nm vs. 100–200 nm) and to the higher efficiency to get endosome escape when LCPs were dissolved in the endosomes, leading to more sustained RNA release in the cytosol. From this report, it appears that it is still necessary to obtain a better understanding of the optimal LDH:DNA ratio parameters for the delivery of functional siRNA using LDH nanoparticles. In this regard, Wu et al. [197] demonstrated that an optimal LDH/gene mass ratio was around 20:1 in terms of cellular uptake amount of gene segments, whereas the ratio was around 5:1 in terms of target gene silencing efficacy in MCF-7 cells. The authors ascribed these interesting results to a reasonable trade-off between DNA loading on the LDHs and dissolution rate. Cellular internalization of LDH NPs is basically driven by clathrin-mediated endocytosis. Once entered into the cells, LDH nanoparticles tend to be dissolved (at higher rate within the endosomes) and release the siRNA. The efficacy of RNA-induced silencing is therefore dependent upon the loading amount of dsDNA/ siRNA per LDH particle, the number of LDH particles, and the suitable release rate of dsDNA/siRNA. The 5:1 ratio seems to be a reasonable compromise between these different factors.

6. LDHs Applications in Cell Biology: From Cellular Differentiation to Cancer Therapy

In general, 2D clay materials have been demonstrated as biocompatible [198,199], suitable systems for synthetic biology [200]. By employing micron sized colloidal objects these compounds have been effectively used for in vitro reconstituting cellular motility [201]. In the specific case of LDHs, these clays are starting to be more and more investigated as to their direct interaction with living cells [202,203].

In particular, the toxicity of LDHs to cells has been thoroughly investigated [204]. As expected from other types of clays, their toxicity potential is dose and time dependent with particle sizes, their shapes and surface charge being determinant features for cellular uptakes. The reticular endothelial system is able to sequestrate LDHs systems, especially those with sizes greater than 50 nm. Notably, LDHs with sizes between 50 and 200 nm show concentration dependent uptake, whereas sizes 350 nm and above are not concentration dependent [205]. LDHs enter cells through endocytotic pathway; however the hexagonal shaped LDH crystallite was found to be distributed within the nucleus of the cells [205]. These results suggested the promising drug delivery potential of LDH at the cellular level without damaging cell structure. In the biofluids, LDHs produce some tissue and cell friendlily by-products (H_2O, Mg^{2+}, Al^{3+}, Zn^{2+}) under physiological conditions [206]. In turn, this effect can mitigate the acidification tendencies in endosomes and lysosome of cells after the nanocomposite uptake, ultimately leading to a sustained and pH dependent drug release that is also beneficial for reducing drug toxicity [204].

6.1. Cellular Differentiation

In a very recent work, LDHs have been reported as a promising material for bioengineering application, showing that LDH nanomaterials modulate cell adhesion, proliferation, and migration and demonstrating their suitability in the biomaterial field and in the specific context of tissue bioengineering [207]. In the following, LDH interaction with cells will be investigated focusing on the biocompatibility, the latest applications in cellular differentiation, and the applications in cancer therapy. A specific investigation regarding the LDH biocompatibility was recently carried out by Cunha et al. [208]. In their research, adult female Wistar rats were subjected to the intramuscular implantation of two types of LDHs of magnesium/ aluminum (Mg_2Al-Cl) and zinc/ aluminum (Zn_2Al-Cl). Interestingly, the LDHs did not lead to any sign of inflammatory reactions; on the contrary, they promoted collagen adsorption. More specifically, Mg_2Al-Cl promoted multiple collagen invaginations (mostly collagen type-I), whereas Zn_2Al-Cl induced collagen type–III. Li et al. reported on the fabrication of layered double hydroxide/poly-dopamine composite coating with surface heparinization onto Mg alloys for application in endothelialization and hemocompatibility [209]. The LDHs were directly grown onto the Mg sample by reported hydrothermal methods [210] in which Mg alloy plates are placed in a Teflon liner which contain an aluminum nitrate solution at 120 °C for 12 h. The MgAl LDH was then coated with poly-dopamine and heparin. The resulting composite material was tested for its corrosion resistance and the ability to enhance, with respect to the bare Mg surface, the adherence, proliferation and migration rate of the human umbilical vein endothelial cells and inhibited the platelets adhesion.

The interaction between cells and nanomaterials can be employed for tuning differentiation switches of stem cells, according to precise biomechanical or biochemical triggers [211,212]. LDHs were demonstrated as biocompatible materials by Ramanathan et al. [213]. In their experiments, they prepared Poly(3-Hydroxybutyric acid)-Poly (N-vinylpyrrolidone) fibers loaded with MgAl LDHs and coated over the hydroxyapatite pellets for the realization of bone grafts; the resulting systems showed good compatibility towards MG63 human osteosarcoma 3AB-OS cancer stem cell lines. LDH nanocomposites with arginylglycylaspartic acid and kartogenin were incorporated into a gel together with tonsil-derived mesenchymal stem cells [214]. Interestingly, the cells were observed to aggregate in the nanocomposite system. By analysis of mRNA content, chondrogenic biomarkers of type II collagen and transcription factor SOX 9 significantly increased, ultimately facilitating a chondrogenic differentiation.

In a more in-depth investigation, Kang et al. [215] studied the effect of MgAl LDHs and ZnAl LDHs in promoting the dynamic expression of genes in osteogenic differentiation pathways. LDHs determined a cytoskeleton rearrangement on the pre-osteoblasts, dependent on the modulating of Cofilin and PP2A phosphorylations, and a significant upmodulation of the osteoblastic classical marker genes (Runt-related transcription factor 2, Osterix, and Osteocalcin), while requiring the activation of c-Jun N-terminal Kinase JNK and extracellular signal–regulated kinases genes. Very recently, a thorough investigation of the LDH-induced inflammatory landscape onto osteoblasts was carried out by da Silva Feltran et al. [216]. In their report, they demonstrated that MgAl LDHs and ZnAl LDHs challenged on the MC3T3-E1 pre-osteoblasts inducing a down-modulation of major pro-inflammatory genes related to cytokines, precisely the tnfα, nfkb, il18, il6, and il1ß genes. On the other hand, an up-modulation of anti-inflammatory cytokines il6, il10, and tgfß genes was observed (see Figure 14). The authors concluded that the effects observed by LDHs could be ascribed to the activation of the Sonic hedgehog signalling in the osteoblasts, permitting the obtaining of a better comprehension of the molecular mechanisms driving the later LDH-induced osteoblast differentiation.

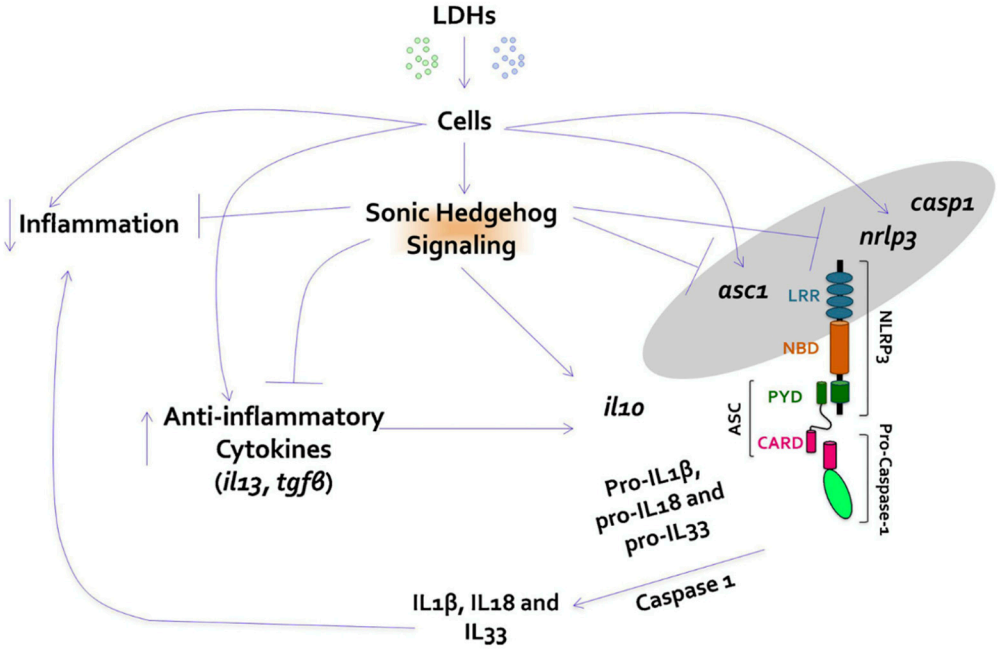

Figure 14. Role of LDHs in inducing the anti-inflammatory Sonic hedgehog acute inflammatory molecular pathway. Reprinted from Ref. [216], Copyright (2019), with permission from Elsevier.

6.2. Contrast Agents

Manganese-based LDHs have been demonstrated as powerful magnetic contrast agents with outstanding pH response and high relaxivity. Indeed, Li et al. [217] reported that, in comparison with free Mn^{2+} ions, the Mn-based LDH systems (prepared from isomorphic substitution from Mg_3Al LDHs) showed a higher longitudinal relaxivity (9.48 mm^{-1} s^{-1} at pH 5.0, and 6.82 mm^{-1} s^{-1} at pH 7.0 vs. 1.16 mm^{-1} s^{-1} at pH 7.4 of free Mn^{2+} ions). Intriguingly, they ascribed these results to the unique microstructural coordination environment surrounding Mn atoms in the Mn LDH framework, as demonstrated by EXAFS measurements. They also observed that the variation of Mn···(OH_2)x coordination in Mn-LDHs in acidic buffer (pH 5.0) led to the excellent T1-weighted magnetic resonance imaging performance. Afterwards, they proved the intracellular uptake of the Mn-LDHs on the B16F10 cancer cells and the outstanding potentiality as in vivo tumor imaging systems (see Figure 15).

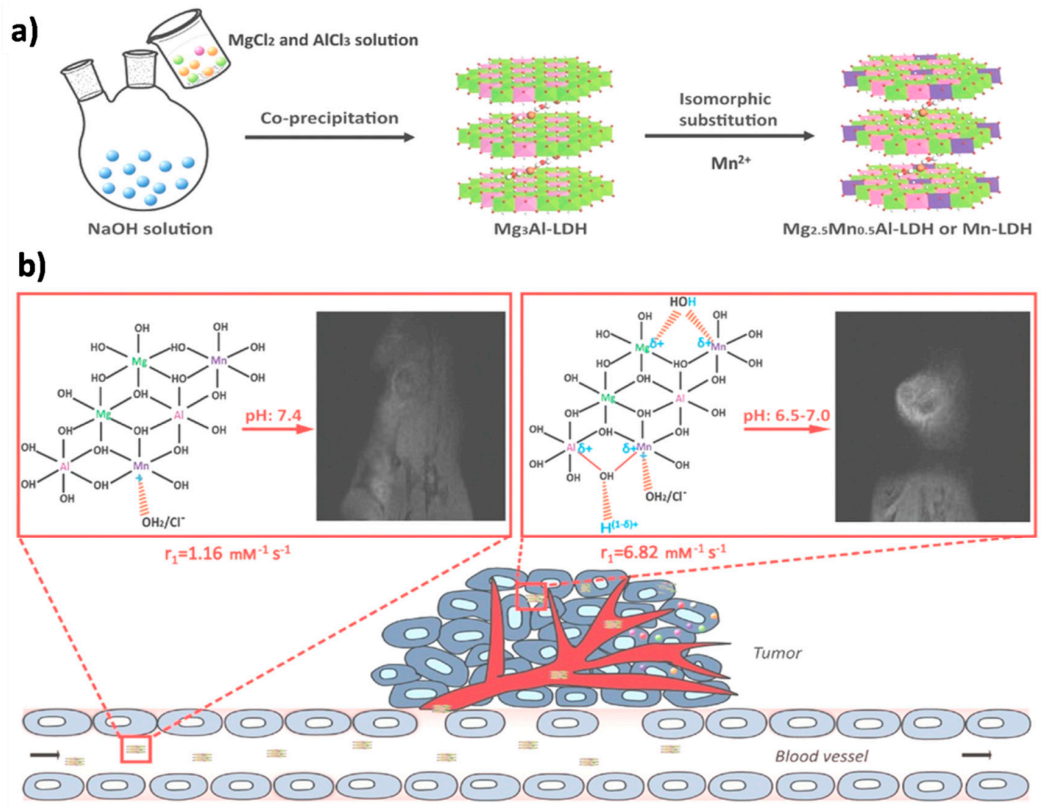

Figure 15. (**a**) Scheme of the $Mg_{2.5}Mn_{0.5}Al$ LDH (Mn-LDH) from co-precipitation and isomorphic substitution. (**b**) Application of the Mn LDH as magnetic contrast agents showing an ultrasensitive pH response and high relaxivity. Reproduced from Ref. [217]. Copyright © 2014 by John Wiley and Sons, Inc. Reprinted with permission from John Wiley and Sons, Inc.

6.3. Drug Delivery

LDHs are reported as very efficient drug nanovehicles [218,219] since, in comparison to other inorganic nanovehicles, including silica and gold nanoparticles, quantum dots, and carbon nanotubes, they are featured with excellent biocompatibility [205], high drug loading capacity [220], and pH-responsive property [221], with biodegradability in the cellular cytoplasm [222]. Such outstanding properties make LDHs an efficient non-viral drug delivery vehicle, and also a reservoir for bioactive or bio-fragile molecules. Note that the intercalated drugs can be released either by deintercalation through anionic exchange with the surrounding anions (such as Cl^- and phosphate), or through the acidic dissolution of LDH hydroxide layers. The predominant mechanism depends on the pH value and the nature of the drug. LDH internalization into cells is mainly carried out by clathrin-mediated endocytosis [223], in which the material to be internalized is surrounded by an area of cell membrane, which buds off inside the cell to form a vesicle containing the ingested material. However, following the reports from Bao et al. [224] for LDH nanosheets-mediated molecular delivery to plant cells, the typical inhibitors of endocytosis and low temperature incubation did not prevent LDH internalization, meaning that the penetration of the plasma membrane can also occur via non-endocytic pathways (see Figure 16).

Many reports have demonstrated the immense potentiality of these materials in drug loading and sustained release. For instance, model antioxidant drugs such as carnosine and gallic acid can be intercalated into MgAl LDHs by ion exchange and coprecipitation. The drugs are released in a pH = 7.4 phosphate buffered saline medium, following a gradual and biphasic release [225]. Drug release from LDHs can be triggered by three different mechanisms: ion exchange, desorption and weathering. Whereas ion exchange only depends on the anion nature, the desorption from LDHs is dependent on the pH of the medium. Taking ibuprofen as a model drug, anion exchange triggers ibuprofen release in

the intestinal medium, whereas surface reactions mediated by solid weathering determine the release in acid media [226]. Many recent examples report on the fabrication of drug-LDHs nanohybrids. Yasaei et al. [227] demonstrated the direct coprecipitation in the presence of simvastatin (a drug used for bone regeneration) and the ion exchange of nitrate and carbonate containing LDHs in a simvastatin solution. The authors found a higher drug loading and more sustained drug releases in the case of nitrate-based LDHs. Bouaziz et al. found similar efficient loading and sustained release of nisin (among the most widely used bacteriocin peptides used in food safety) onto zinc-aluminum LDHs [228]. Similarly, pH-sensitive bead systems composed of folic acid intercalated into LDHs and chitosan represent an ideal drug delivery system for folic acid release at simulated conditions similar to the gastrointestinal tract [229]. Among the possible investigated drug systems, alendronate represents a relevant example, being an anti-resorptive and bone-remodeling drug with poor intracellular permeability, which in turn results in low drug efficacy. In this regard, Piao et al. [230] demonstrated that MgAl LDHs were able to obtain a 10-fold enhancement of the cellular uptake efficacy of alendronate in MG63 cells with respect to the bare alendronate. Notably, LDH itself did not show any effect on proliferation and osteogenic differentiation of MG63 cells (see Figure 17).

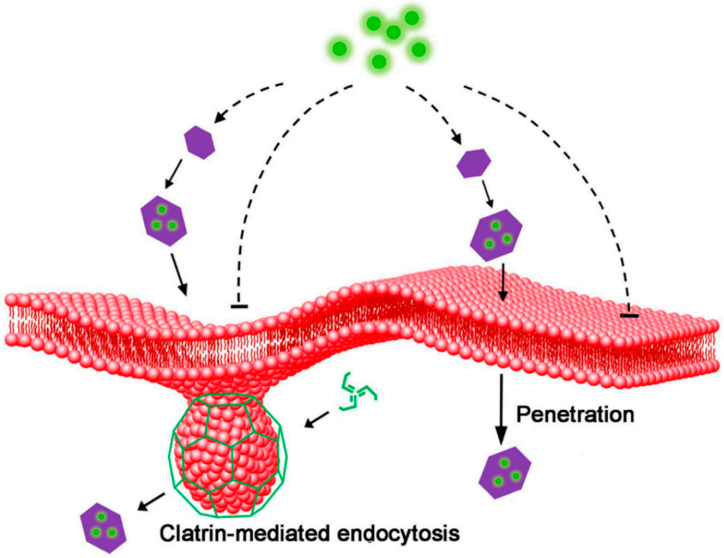

Figure 16. Mechanisms of LDH-lactate internalization (clathrin-mediated endocytosis) for molecule delivery into plant cells. Figure reproduced from Ref. [224] under the terms of the Creative Commons Attribution Non-Commercial License.

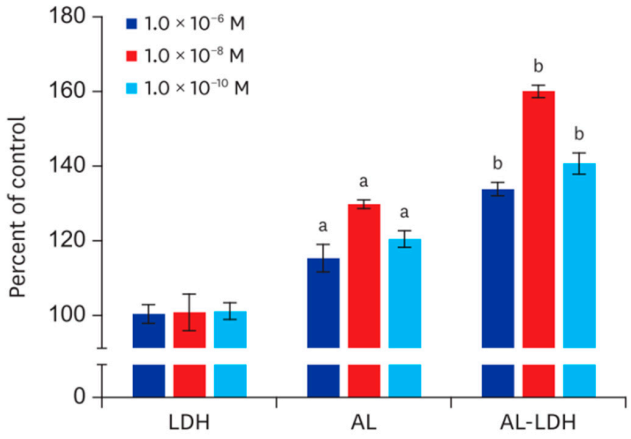

Figure 17. Experimental results showing the biocompatibility of pristine MgAl LDHs (LDH), Alendronate (AL) and Alendronate-LDH nanohybrids (AL-LDH). Figure reproduced from Ref. [230] under the terms of the Creative Commons Attribution Non-Commercial License.

LDHs have also shown important applications in chemotherapy, since they can improve treatment of tumors by facilitating pH-triggered drug delivery. For instance, Khorsandi et al. [231] investigated upon the cellular responses to curcumin-LDH hybrid nanoparticles following a photodynamic treatment of MDA-MB-231 human breast cancer cells. For this purpose, the human breast cancer cells were treated with curcumin-LDH NPs and were then irradiated, demonstrating that the curcumin-LDH hybrid had a cytotoxic and antiprolifrative effect due to the generation of reactive oxygen species, which led to autophagy and apoptosis. Recently, Liu et al. [232] demonstrated a very intriguing pH-triggered hydrazone-carboxylate complex of doxorubicin, a model chemotherapy drug, which was encapsulated in MgAl LDH NPs via a ion-exchange processes. These nanohybrids were internalized by clathrin-dependent endocytosis and then shifted to lysosomes, where hydrazone-Dox complexes were released (due to the low pH of this compartment), ultimately resulting in free cytosolic doxorubicin which in turn facilitated the cell death (MCF-7 and HeLa cells) via cathepsin-mediated cell apoptosis. A more complex drug-nanohybrid was realized by Wen et al. [233] with the aim to produce a pH-triggered drug delivery system consisting of folic-acid (FA) functionalized tellurium nanodots (Te NDs) which were in-situ synthesized in paclitaxel (PTX)-loaded MgAl LDHs. The latter were, in turn, gated onto mesoporous silica nanoparticles (MSNs). The structural properties of the resulting nanosystem were characterized by SEM, XRD, XPS and FT-IR methods. Interestingly, these nanosystems combined the ability of Te nanodots as phototherapeutic agent and the pH-triggered release of paclitaxel to human cervical cancer cells HeLa and human embryonic kidney cells 293T (see Figure 18).

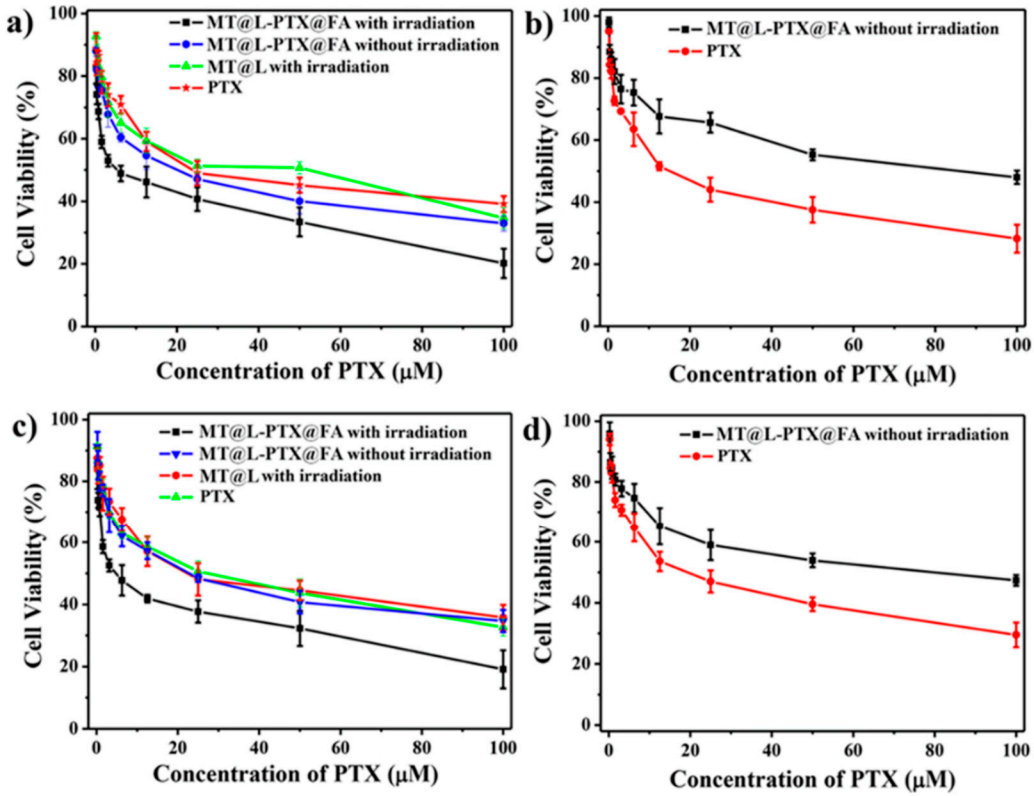

Figure 18. Experimental results showing the cytotoxicity of the hierarchical nanosystem consisting of Te NDs within Paclitaxel-Loaded MgAl LDH gated mesoporous silica NPs towards (**a**) HepG2 cells, and (**c**) HeLa cells for 48 h with or without irradiation. Cytotoxicity of MT@L-PTX@FA without irradiation and free Paclitaxel on (**b**) HL7702 cells, and (**d**) 293T cells for 48 h. Reprinted with permission from Ref. [233]. Copyright (2019) American Chemical Society.

CaAl LDHs have shown useful properties as a drug delivery system for methotrexate to MG-63 human osteosarcoma cell line [234]. Remarkably, CaAl LDHs alone have been recently demonstrated as an active anticancer agent, owing to the involvement of Ca^{2+} ion with the CAMKIIα protein and associated SOD activity in cancer cell [235]. The results by Bhattacharjeeet al. exhibited significant down regulation of CAMKIIα and SOD gene by CaAl LDHs at cellular level, leading to apoptosis of the cancer cell. Exfoliated ultrathin MgAl LDHs prepared by a single-step procedure in presence of formamide [236] can be used as a confinement matrix of carbon nanodots (CDs), allowing for an enhancement of fluorescence lifetime of CDs. In turn, this leads to an improvement of their efficacy in photoacoustic imaging performance and tumor inhibition under the 808 nm irradiation [237] in Hela tumor-models consisting of male nude Balb/c mice.

LDHs have also been demonstrated as an effective drug delivery system of etoposide, a chemotherapeutic agent for the treatment of a number of diseases, including glioblastoma, one of the most common and lethal intrinsic brain tumors. Wang et al. [238] incorporated etoposide into LDH nanoparticles in order to overcome the inherent drug resistant problem, such as poor tumor selectivity, and low solubility in water, permitting to significantly facilitate uptake by glioblastoma cells and enhance apoptosis efficiency, self-renewal repression, and epithelial-mesenchymal transition program reversion. The authors conducted a profound transcriptomic analysis to find the role of different protein pathways involved in the delivery of etoposide into glioblastoma cells, including PI3K–AKt, downstream mTOR, Nuclear factor kappa B (NF-κB), mitochondrial Bcl-2, activated caspase, and Wnt-β-catenin signaling (see Figure 19).

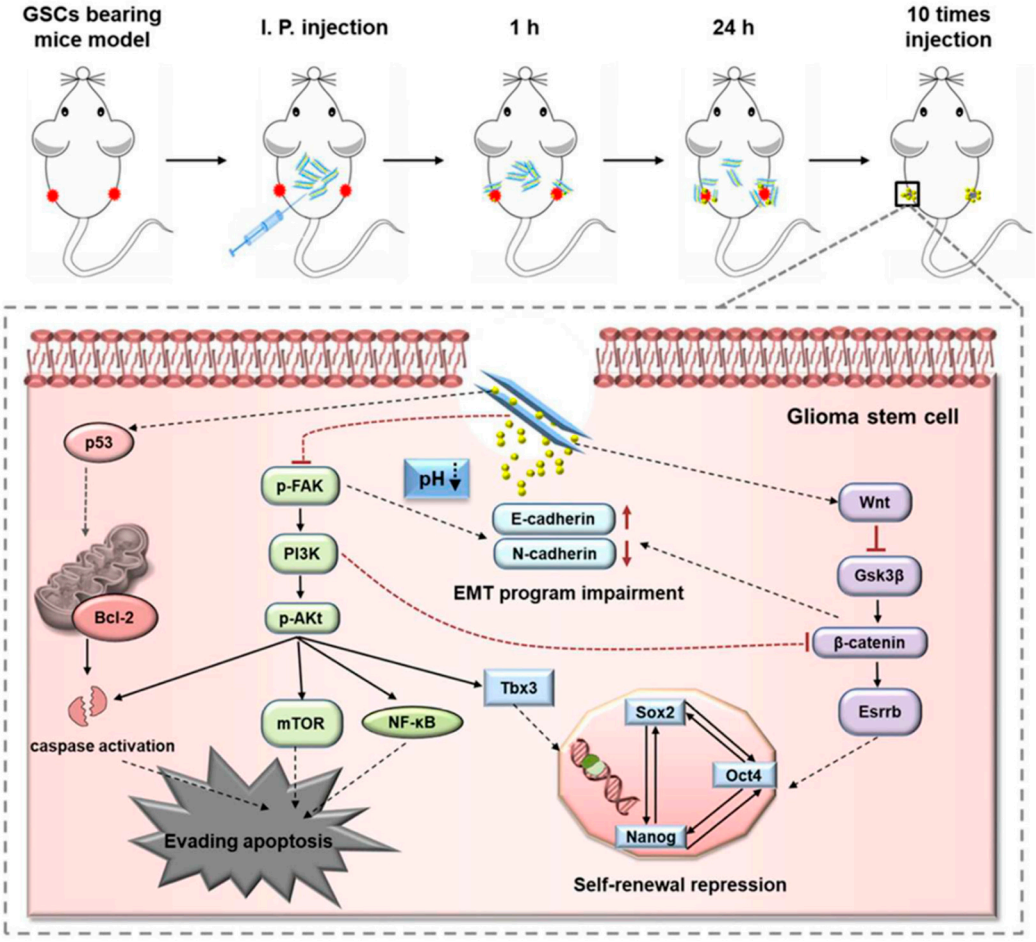

Figure 19. Molecular mechanisms involved in etoposide LDH NPs reversing chemoresistance and eradicating human glioma stem cells. Republished with permission from the Royal Society of Chemistry, from Ref. [238]; permission conveyed through Copyright Clearance Center, Inc.

A different scenario has been elicited as it concerns antibiotics loading. Model antibiotics such as tetracycline and oxytetracyline [239] were shown not to be intercalated into LDHs, but more likely to be adsorbed on their external surface and released according to a Fickian diffusion model. The LDHs adsorbed antibiotics are still active towards *E. coli* and *S. epidermis*, showing a decrease of efficacy in comparison to the free molecules. Among the recent applications in anticancer drug delivery, Asiabi et al. [240] prepared a novel biocompatible pseudo-hexagonal NaCa-layered double metal hydroxides (see Figure 20), which allowed for a sustained pH-triggered release of dacarbazine. This system allowed for enhanced anticancer activity in malignant melanoma cells (malignant A-375 melanoma and breast cancer MCF-7 cell lines) at higher values in comparison to the free drug [240]. Similarly, Shahabadi et al. [241] demonstrated the suitability of Fe_3O4@CaAl-LDHs as levodopa delivery systems for Mel-Rm Cells Melanoma (NCIt: C3224) cells, permitting improvement in the efficacy of the free drug, owing to a pH-triggered release mechanism.

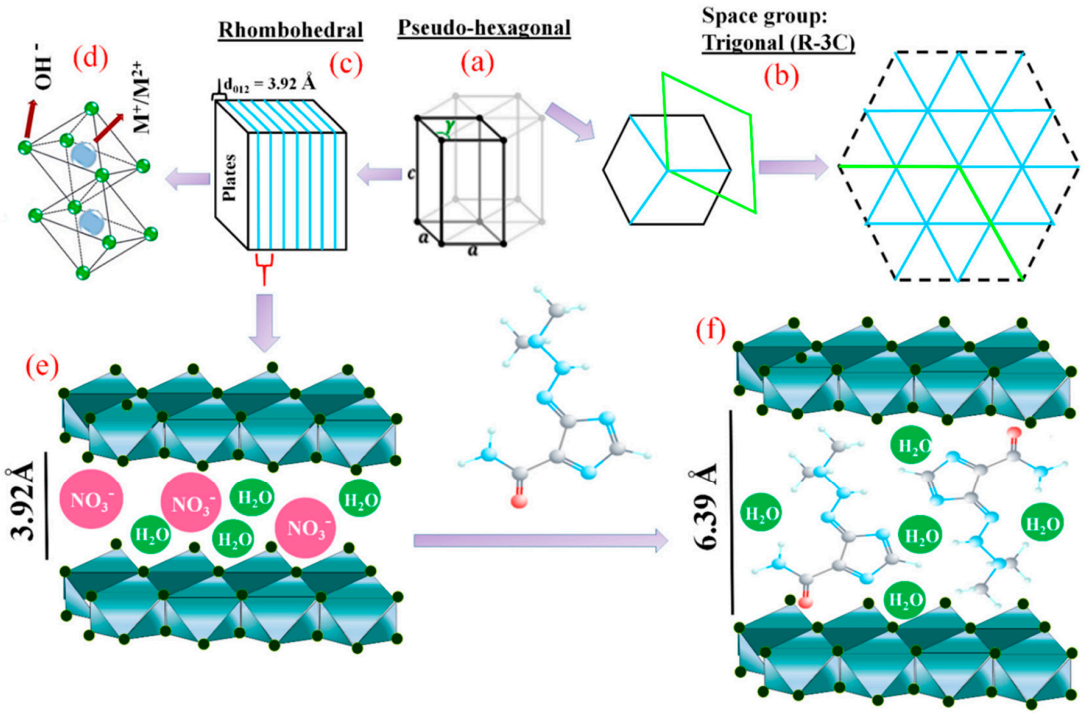

Figure 20. Schematic illustration of the structure of NaCa LDH for dacarbazine drug loading. NaCa LDH has (**a**) pseudo-hexagonal (P-3m1) structure with (**b**) a trigonal crystal structure (R-3C) and (**c**) rhombohedral lattice system. (**d**) The M^{2+}/M^{+} ions are surrounded approximately octahedrally by hydroxide ions, (**e**) structure of NO_3LDH, and (**f**) structure of the LDH intercalated with dacarbazine drug, showing an enlargement of the inter-layer spacing. Reprinted from Ref. [240], with permission from Elsevier.

7. Conclusions

The aim of this review is to provide the reader with a fresh view in the field of LDH applications in chemistry and biology. As for the chemistry-related applications, LDHs are a definitely promising platform for organics catalysis and photocatalysis. Their main advantages lie in the low cost, mild, eco-compatible, low temperature synthetic approaches in controlled reaction environments (i.e., the interlamellar space), along with the possibility to recycle the LDHs after their employment. However, a specific issue of these materials is the "trails and error" approach that typically characterizes the literature of these materials for chemistry-applications. In the future, a more predictive approach towards the understanding of the reaction mechanisms involving the metal centers forming the LDHs would highly benefit the development of this research field. As for the biology-related applications,

LDHs have proved to be a suitable material for drug and nucleic acid delivery, due to their partially positive charge that greatly facilitates cellular uptake by electrostatic forces. We have focused on the novel still poor explored applications in DNA and siRNA delivery, where LDHs are able to play a key role given their biocompatibility and easy synthesis and loading approaches. Still, many new investigations are needed in the field of interactions with cells (especially stem cells and also cancer cells), with the aim to precisely understand the intracellular molecular pathways that can be activated by the interaction of LDHs with cells.

This overview on LDHs considers only a portion of the numerous organic reactions protocols which could benefit of LDHs catalytic properties as well as only some remarkable examples among the different applications of these materials in the field of drug delivery and advanced medical therapies. While this study does not pretend to detail all the literature actually available, the authors hope that the most important and recent achievements have been reviewed, with the ultimate goal to offer a panoramic vision of the importance and potential of this branch of chemistry in between material science, organic synthesis and biology.

Author Contributions: Methodology, G.P., A.O., A.M., G.A., and A.B.; writing—original draft preparation, G.A., A.B.; writing—review and editing, G.P. and E.M.; supervision, E.M., B.P. and P.G.M.

Funding: This research received no external funding.

Acknowledgments: The authors acknowledge ATeN center (Unipa) for hospitality and support.

Conflicts of Interest: The authors declare no conflict of interest.

References

1. Tiwari, J.N.; Tiwari, R.N.; Kim, K.S. Zero-dimensional, one-dimensional, two-dimensional and three-dimensional nanostructured materials for advanced electrochemical energy devices. *Prog. Mater. Sci.* **2012**, *57*, 724–803. [CrossRef]
2. Sciortino, A.; Mauro, N.; Buscarino, G.; Sciortino, L.; Popescu, R.; Schneider, R.; Giammona, G.; Gerthsen, D.; Cannas, M.; Messina, F. β-C_3N_4 Nanocrystals: Carbon Dots with Extraordinary Morphological, Structural, and Optical Homogeneity. *Chem. Mater.* **2018**, *30*, 1695–1700. [CrossRef]
3. Miccichè, C.; Arrabito, G.; Amato, F.; Buscarino, G.; Agnello, S.; Pignataro, B. Inkjet printing Ag nanoparticles for SERS hot spots. *Anal. Methods* **2018**, *10*, 3215–3223. [CrossRef]
4. Cataldo, S.; Salice, P.; Menna, E.; Pignataro, B. Carbon nanotubes and organic solar cells. *Energy Environ. Sci.* **2012**, *5*, 5919–5940. [CrossRef]
5. Fang, Y.; Jiang, Y.; Acaron Ledesma, H.; Yi, J.; Gao, X.; Weiss, D.E.; Shi, F.; Tian, B. Texturing Silicon Nanowires for Highly Localized Optical Modulation of Cellular Dynamics. *Nano Lett.* **2018**, *18*, 4487–4492. [CrossRef]
6. Arrabito, G.; Errico, V.; Zhang, Z.; Han, W.; Falconi, C. Nanotransducers on printed circuit boards by rational design of high-density, long, thin and untapered ZnO nanowires. *Nano Energy* **2018**, *46*, 54–62. [CrossRef]
7. Errico, V.; Arrabito, G.; Plant, S.R.; Medaglia, P.G.; Palmer, R.E.; Falconi, C. Chromium inhibition and size-selected Au nanocluster catalysis for the solution growth of low-density ZnO nanowires. *Sci. Rep.* **2015**, *5*, 12336. [CrossRef]
8. Kim, K.S.; Zhao, Y.; Jang, H.; Lee, S.Y.; Kim, J.M.; Kim, K.S.; Ahn, J.-H.; Kim, P.; Choi, J.-Y.; Hong, B.H. Large-scale pattern growth of graphene films for stretchable transparent electrodes. *Nature* **2009**, *457*, 706–710. [CrossRef]
9. Pradhan, D.; Leung, K.T. Vertical growth of two-dimensional zinc oxide nanostructures on ITO-coated glass: Effects of deposition temperature and deposition time. *J. Phys. Chem. C* **2008**, *112*, 1357–1364. [CrossRef]
10. Jeevanandam, J.; Barhoum, A.; Chan, Y.S.; Dufresne, A.; Danquah, M.K. Review on nanoparticles and nanostructured materials: History, sources, toxicity and regulations. *Beilstein J. Nanotechnol.* **2018**, *9*, 1050–1074. [CrossRef]
11. Wang, Q.; O'Hare, D. Recent Advances in the Synthesis and Application of Layered Double Hydroxide (LDH) Nanosheets. *Chem. Rev.* **2012**, *112*, 4124–4155. [CrossRef] [PubMed]
12. Crepaldi, E.L.; Pavan, P.C.; Valim, J.B. Comparative Study of the Coprecipitation Methods for the Preparation of Layered Double Hydroxides. *J. Braz. Chem. Soc.* **2000**, *11*, 64–70. [CrossRef]

13. Bukhtiyarova, M.V. A review on effect of synthesis conditions on the formation of layered double hydroxides. *J. Solid State Chem.* **2019**, *269*, 494–506. [CrossRef]
14. Mishra, G.; Dash, B.; Pandey, S. Layered double hydroxides: A brief review from fundamentals to application as evolving biomaterials. *Appl. Clay Sci.* **2018**, *153*, 172–186. [CrossRef]
15. Guo, X.; Zhang, F.; Evans, D.G.; Duan, X. Layered double hydroxide films: Synthesis, properties and applications. *Chem. Commun.* **2010**, *46*, 5197–5210. [CrossRef] [PubMed]
16. Liu, B.J.; Li, Y.; Huang, X.; Li, G.; Li, Z. Layered Double Hydroxide Nano- and Microstructures Grown Directly on Metal Substrates and Their Calcined Products for Application as Li-Ion Battery Electrodes. *Adv. Funct. Mater.* **2008**, *18*, 1448–1458. [CrossRef]
17. Liu, J.; Huang, X.; Li, Y.; Sulieman, K.M.; He, X.; Sun, F. Facile and Large-Scale Production of ZnO/Zn−Al Layered Double Hydroxide Hierarchical Heterostructures. *J. Phys. Chem. B* **2006**, *110*, 21865–21872. [CrossRef] [PubMed]
18. Guo, X.; Xu, S.; Zhao, L.; Lu, W.; Zhang, F.; Evans, D.G.; Duan, X. One-Step Hydrothermal Crystallization of a Layered Double Hydroxide/Alumina Bilayer Film on Aluminum and Its Corrosion Resistance Properties. *Langmuir* **2009**, *25*, 9894–9897. [CrossRef]
19. Scarpellini, D.; Leonardi, C.; Mattoccia, A.; Di Giamberardino, L.; Medaglia, P.G.; Mantini, G.; Gatta, F.; Giovine, E.; Foglietti, V.; Falconi, C.; et al. Solution-Grown Zn/Al Layered Double Hydroxide Nanoplatelets onto Al Thin Films: Fine Control of Position and Lateral Thickness. *J. Nanomater.* **2015**, *2015*, 1–8. [CrossRef]
20. Polese, D.; Mattoccia, A.; Giorgi, F.; Pazzini, L.; Ferrone, A.; Di Giamberardino, L.; Maiolo, L.; Pecora, A.; Convertino, A.; Fortunato, G.; et al. Layered Double Hydroxides intercalated with chlorine used as low temperature gas sensors. *Procedia Eng.* **2015**, *120*, 1175–1178. [CrossRef]
21. Meng, F.; Li, L.; Liang, H.; Xiu, L.; Forticaux, A.; Wang, Z.; Cabán-Acevedo, M.; Jin, S. Hydrothermal Continuous Flow Synthesis and Exfoliation of NiCo Layered Double Hydroxide Nanosheets for Enhanced Oxygen Evolution Catalysis. *Nano Lett.* **2015**, *15*, 1421–1427.
22. Zhou, Y.; Li, X.; Wang, K.; Hu, F.; Zhai, C.; Wang, X. Enhanced photoluminescence emission and surface fl uorescence response of morphology controllable nano porous anodize alumina Zn-Al LDH film. *J. Alloys Compd.* **2019**, *770*, 6–16. [CrossRef]
23. Teixeira, A.C.; Morais, A.F.; Silva, I.G.N.; Breynaert, E.; Mustafa, D. Luminescent Layered Double Hydroxides Intercalated with an Anionic Photosensitizer via the Memory Effect. *Crystals* **2019**, *9*, 153. [CrossRef]
24. Richetta, M.; Digiamberardino, L.; Mattoccia, A.; Medaglia, P.G.; Montanari, R.; Pizzoferrato, R.; Scarpellini, D.; Varone, A.; Kaciulis, S.; Mezzi, A.; et al. Surface spectroscopy and structural analysis of nanostructured multifunctional (Zn, Al) layered double hydroxides. *Surf. Interface Anal.* **2016**, *48*, 514–518. [CrossRef]
25. Kruissink, E.C.; Van Reijen, L.L.; Ross, J.R.H. Coprecipitated nickel-alumina catalysts for methanation at high temperature. Part 1.—Chemical composition and structure of the precipitates. *J. Chem. Soc. Faraday Trans. 1 Phys. Chem. Condens. Phases* **1981**, *77*, 649–663. [CrossRef]
26. Reichle, W.T. Catalytic Reactions by Thermally Activated, Synthetic, Anionic Clay Minerals. *J. Catal.* **1985**, *94*, 547–557. [CrossRef]
27. Martin, K.J.; Pinnavaia, T.J. Layered Double Hydroxides as Supported Anionic Reagents. Halide Ion Reactivity in $[Zn_2Cr(OH)6X.nH_2O]$ (X = Cl, I). *J. Am. Chem. Soc.* **1986**, *108*, 541–542.
28. Zhao, M.Q.; Zhang, Q.; Huang, J.Q.; Wei, F. Hierarchical nanocomposites derived from nanocarbons and layered double hydroxides-Properties, synthesis, and applications. *Adv. Funct. Mater.* **2012**, *22*, 675–694. [CrossRef]
29. Fan, G.; Li, F.; Evans, D.G.; Duan, X. Catalytic applications of layered double hydroxides: Recent advances and perspectives. *Chem. Soc. Rev.* **2014**, *43*, 7040–7066. [CrossRef] [PubMed]
30. Feng, J.; He, Y.; Liu, Y.; Du, Y.; Li, D. Supported catalysts based on layered double hydroxides for catalytic oxidation and hydrogenation: General functionality and promising application prospects. *Chem. Soc. Rev.* **2015**, *44*, 5291–5319. [CrossRef]
31. Newman, S.P.; Jones, W. Synthesis, characterization and applications of layered double hydroxides containing organic guests. *New J. Chem.* **1998**, *22*, 105–115. [CrossRef]
32. Leroux, F.; Taviot-Guého, C. Fine tuning between organic and inorganic host structure: New trends in layered double hydroxide hybrid assemblies. *J. Mater. Chem.* **2005**, *15*, 3628–3642. [CrossRef]
33. Rives, V.; Ulibarri, M.A. Layered double hydroxides (LDH) intercalated with metal coordination compounds and oxometalates. *Coord. Chem. Rev.* **1999**, *181*, 61–120. [CrossRef]

34. Omwoma, S.; Chen, W.; Tsunashima, R.; Song, Y.F. Recent advances on polyoxometalates intercalated layered double hydroxides: From synthetic approaches to functional material applications. *Coord. Chem. Rev.* **2014**, *258–259*, 58–71. [CrossRef]
35. Vicente, R. Characterisation of layered double hydroxides and their decomposition products. *Mater. Chem. Phys.* **2002**, *75*, 19–25.
36. Xu, Z.P.; Zhang, J.; Adebajo, M.O.; Zhang, H.; Zhou, C. Catalytic applications of layered double hydroxides and derivatives. *Appl. Clay Sci.* **2011**, *53*, 139–150. [CrossRef]
37. Auer, S.M.; Gredig, S.V.; Köppel, R.A.; Baiker, A. Synthesis of methylamines from CO_2, H_2 and NH_3 over Cu-Mg-Al mixed oxides. *J. Mol. Catal. A Chem.* **1999**, *141*, 193–203. [CrossRef]
38. Christensen, K.O.; Chen, D.; Lødeng, R.; Holmen, A. Effect of supports and Ni crystal size on carbon formation and sintering during steam methane reforming. *Appl. Catal. A Gen.* **2006**, *314*, 9–22. [CrossRef]
39. Liu, H.; Wierzbicki, D.; Debek, R.; Motak, M.; Grzybek, T.; Da Costa, P.; Gálvez, M.E. La-promoted Ni-hydrotalcite-derived catalysts for dry reforming of methane at low temperatures. *Fuel* **2016**, *182*, 8–16. [CrossRef]
40. Li, P.; Yu, F.; Altaf, N.; Zhu, M.; Li, J.; Dai, B.; Wang, Q. Two-dimensional layered double hydroxides for reactions of methanation and methane reforming in C1 chemistry. *Materials* **2018**, *11*, 221. [CrossRef]
41. Gawande, M.B.; Pandey, R.K.; Jayaram, R.V. Role of mixed metal oxides in catalysis science—Versatile applications in organic synthesis. *Catal. Sci. Technol.* **2012**, *2*, 1113–1125. [CrossRef]
42. Tkatchenko, I. Synthesis with Carbon Monoxide and a Petroleum Product. *Compr. Organomet. Chem.* **2006**, *8*, 101–223.
43. Marchi, A.J.; Apesteguía, C.R. Impregnation-induced memory effect of thermally activated layered double hydroxides. *Appl. Clay Sci.* **1998**, *13*, 35–48. [CrossRef]
44. Rocha, J.; Del Arco, M.; Rives, V.; Ulibarri, M.A. Reconstruction of layered double hydroxides from calcined precursors: A powder XRD and ^{27}Al MAS NMR study. *J. Mater. Chem.* **1999**, *9*, 2499–2503. [CrossRef]
45. Stanimirova, T.S.; Kirov, G.; Dinolova, E. Mechanism of hydrotalcite regeneration. *J. Mater. Sci. Lett.* **2001**, *20*, 453–455. [CrossRef]
46. Erickson, K.L.; Bostrom, T.E.; Frost, R.L. A study of structural memory effects in synthetic hydrotalcites using environmental SEM. *Mater. Lett.* **2005**, *59*, 226–229. [CrossRef]
47. Duan, X.; Lu, J.; Evans, D.G.; Wei, X.; Chen, J.S. Functional Host-Guest Materials. In *Modern Inorganic Synthetic Chemistry: Second Edition*; Elsevier: Amsterdam, The Netherlands, 2017; pp. 493–543. ISBN 9780444635914.
48. Meyn, M.; Beneke, K.; Lagaly, G. Anion-Exchange Reactions of Layered Double Hydroxides. *Inorg. Chem.* **1990**, *29*, 5201–5207. [CrossRef]
49. Radha, A.V.; Kamath, P.V.; Shivakumara, C. Mechanism of the anion exchange reactions of the layered double hydroxides (LDHs) of Ca and Mg with Al. *Solid State Sci.* **2005**, *7*, 1180–1187. [CrossRef]
50. Prasanna, S.V.; Kamath, P.V. Anion-exchange reactions of layered double hydroxides: Interplay between coulombic and h-bonding interactions. *Ind. Eng. Chem. Res.* **2009**, *48*, 6315–6320. [CrossRef]
51. Debecker, D.P.; Gaigneaux, E.M.; Busca, G. Exploring, tuning, and exploiting the basicity of hydrotalcites for applications in heterogeneous catalysis. *Chem. Eur. J.* **2009**, *15*, 3920–3935. [CrossRef]
52. Evans, D.G.; Slade, R.C.T. Structure & Bonding, Chapter Structural Aspects of Layered Double Hydroxides. *Struct. Bond.* **2006**, *119*, 1–87.
53. Sideris, P.J.; Nielsen, U.G.; Gan, Z.; Grey, C.P. Mg/Al Ordering in Layered Double Hydroxides Revealed by Multinuclear NMR Spectroscopy. *Science* **2008**, *321*, 113–117. [CrossRef] [PubMed]
54. Cadars, S.; Layrac, G.; Gérardin, C.; Deschamps, M.; Yates, J.R.; Tichit, D.; Massiot, D. Identification and Quantification of Defects in the Cation Ordering in Mg/Al Layered Double Hydroxides. *Chem. Mater.* **2011**, *23*, 2821–2831. [CrossRef]
55. Sideris, P.J.; Blanc, F.; Gan, Z.; Grey, C.P. Identification of Cation Clustering in Mg–Al Layered Double Hydroxides Using Multinuclear Solid State Nuclear Magnetic Resonance Spectroscopy. *Chem. Mater.* **2012**, *24*, 2449–2461. [CrossRef]
56. Manohara, G.V.; Prasanna, S.V.; Kamath, P.V. Structure and Composition of the Layered Double Hydroxides of Mg and Fe: Implications for Anion-Exchange Reactions. *Eur. J. Inorg. Chem.* **2011**, *2011*, 2624–2630. [CrossRef]
57. Xu, M.; Wei, M. Layered Double Hydroxide-Based Catalysts: Recent Advances in Preparation, Structure, and Applications. *Adv. Funct. Mater.* **2018**, *28*, 1802943. [CrossRef]

58. Hernández, W.Y.; Lauwaert, J.; Van Der Voort, P.; Verberckmoes, A. Recent advances on the utilization of layered double hydroxides (LDHs) and related heterogeneous catalysts in a lignocellulosic-feedstock biorefinery scheme. *Green Chem.* **2017**, *19*, 5269–5302. [CrossRef]
59. Kim, D.; Huang, C.; Lee, H.; Han, I.; Kang, S.; Kwon, S.; Lee, J.; Han, Y.; Kim, H. Hydrotalcite-type catalysts for narrow-range oxyethylation of 1-dodecanol using ethyleneoxide. *Appl. Catal. A Gen.* **2003**, *249*, 229–240. [CrossRef]
60. Constantino, V.R.L.; Pinnavaia, T.J. Basic Properties of $Mg^{2+}1-xAl^{3+}x$ Layered Double Hydroxides Intercalated by Carbonate, Hydroxide, Chloride, and Sulfate Anions. *Inorg. Chem.* **1995**, *34*, 883–892. [CrossRef]
61. Lü, Z.; Zhang, F.; Lei, X.; Yang, L.; Xu, S.; Duan, X. In situ growth of layered double hydroxide films on anodic aluminum oxide/aluminum and its catalytic feature in aldol condensation of acetone. *Chem. Eng. Sci.* **2008**, *63*, 4055–4062. [CrossRef]
62. Sels, B.F.; De Vos, D.E.; Jacobs, P.A. Hydrotalcite-like anionic clays in catalytic organic reactions. *Catal. Rev. Sci. Eng.* **2001**, *43*, 443–488. [CrossRef]
63. Cirujano, F.G. Engineered MOFs and Enzymes for the Synthesis of Active Pharmaceutical Ingredients. *ChemCatChem* **2019**. [CrossRef]
64. Krow, G.R. The Baeyer-Villiger Oxidation of Ketones and Aldehydes. *Org. React.* **2004**, *43*, 251–798.
65. Baeyer, A.; Villiger, V. Ueber die Einwirkung des Caro'schen Reagens auf Ketone. *Z. Anal. Chem.* **1902**, *41*, 765–766. [CrossRef]
66. Renz, M.; Meunier, B. MICROREVIEW 100 Years of Baeyer–Villiger Oxidations. *Eur. Hournal Org. Chem.* **1999**, *1999*, 737–750. [CrossRef]
67. Fried, J.; Thoma, R.W.; Klingsberg, A. Oxidation of steroids by micro örganisms. iii. side chain degradation, ring d-cleavage and dehydrogenation in ring a. *J. Am. Chem. Soc.* **1953**, *75*, 5764–5765. [CrossRef]
68. Mihovilovic, M.D.; Rudroff, F.; Winninger, A.; Schneider, T.; Schulz, F.; Reetz, M.T. Microbial Baeyer−Villiger Oxidation: Stereopreference and Substrate Acceptance of Cyclohexanone Monooxygenase Mutants Prepared by Directed Evolution. *Org. Lett.* **2006**, *8*, 1221–1224. [CrossRef]
69. ten Brink, G.-J.; Arends, I.W.C.E.; Sheldon, R.A. The Baeyer−Villiger Reaction: New Developments toward Greener Procedures. *Chem. Rev.* **2004**, *104*, 4105–4124. [CrossRef] [PubMed]
70. Leisch, H.; Morley, K.; Lau, P.C.K. Correction to Baeyer-Villiger Monooxygenases: More Than Just Green Chemistry. *Chem. Rev.* **2013**, *113*, 5700. [CrossRef]
71. Kaneda, K.; Ueno, S.; Imanaka, T. Heterogeneous Baeyer-Villiger Oxidation of Ketones Using an Oxidant Consisting of Molecular Oxygen and Aldehydes in the Presence of Hydrotalcite Catalysts. *J. Chem. Soc. Chem. Commun.* **1994**, *25*, 797–798. [CrossRef]
72. Kaneda, K.; Ueno, S.; Imanaka, T. Catalysis of transition metal-functionalized hydrotalcites for the Baeyer-Villiger oxidation of ketones in the presence of molecular oxygen and benzaldehyde. *J. Mol. Catal. A. Chem.* **1995**, *102*, 135–138. [CrossRef]
73. Kawabata, T.; Fujisaki, N.; Shishido, T.; Nomura, K.; Sano, T.; Takehira, K. Improved Fe/Mg-Al hydrotalcite catalyst for Baeyer-Villiger oxidation of ketones with molecular oxygen and benzaldehyde. *J. Mol. Catal. A Chem.* **2006**, *253*, 279–289. [CrossRef]
74. Kaneda, K.; Yamashita, T. Heterogeneous Baeyer-Viiliger Oxidation of Ketones Using m-Chloroperbenzoic Acid Catalyzed by Hydrotaicites. *Tetrahedron Lett.* **1996**, *37*, 4555–4558. [CrossRef]
75. Pillai, U.R.; Sahle-Demessie, E. Sn-exchanged hydrotalcites as catalysts for clean and selective Baeyer-Villiger oxidation of ketones using hydrogen peroxide. *J. Mol. Catal. A Chem.* **2003**, *191*, 93–100. [CrossRef]
76. Jiménez-Sanchidrián, C.; Hidalgo, J.M.; Llamas, R.; Ruiz, J.R. Baeyer-Villiger oxidation of cyclohexanone with hydrogen peroxide/benzonitrile over hydrotalcites as catalysts. *Appl. Catal. A Gen.* **2006**, *312*, 86–94. [CrossRef]
77. Olszówka, J.; Karcz, R.; Napruszewska, B.D.; Duraczyńska, D.; Gaweł, A.; Bahranowski, K.; Serwicka, E.M. Baeyer-Villiger oxidation of cyclohexanone with H_2O_2/acetonitrile over hydrotalcite-like catalysts: Effect of Mg/Al ratio on the ε-caprolactone yield. *Catal. Commun.* **2017**, *100*, 196–201. [CrossRef]
78. Olszówka, J.E.; Karcz, R.; Napruszewska, B.D.; Michalik-Zym, A.; Duraczyńska, D.; Kryściak-Czerwenka, J.; Niecikowska, A.; Bahranowski, K.; Serwicka, E.M. Effect of Mg–Al hydrotalcite crystallinity on catalytic Baeyer-Villiger oxidation of cyclohexanone with H_2O_2/acetonitrile. *Catal. Commun.* **2018**, *107*, 48–52. [CrossRef]

79. Olszówka, J.E.; Karcz, R.; Michalik-Zym, A.; Napruszewska, B.D.; Bielańska, E.; Kryściak-Czerwenka, J.; Socha, R.P.; Nattich-Rak, M.; Krzan, M.; Klimek, A.; et al. Effect of grinding on the physico-chemical properties of Mg-Al hydrotalcite and its performance as a catalyst for Baeyer-Villiger oxidation of cyclohexanone. *Catal. Today* **2018**, *333*, 147–153. [CrossRef]
80. Jones, G. The Knoevenagel Condensation. In *Organic Reactions*; Major Reference Works; John Wiley & Sons, Inc.: New York, NY, USA, 2011; ISBN 9780471264187.
81. Touré, B.B.; Hall, D.G. Natural Product Synthesis Using Multicomponent Reaction Strategies. *Chem. Rev.* **2009**, *109*, 4439–4486. [CrossRef]
82. Yamashita, S.; Iso, K.; Kitajima, K.; Himuro, M.; Hirama, M. Total Synthesis of Cortistatins A and J. *J. Org. Chem.* **2011**, *76*, 2408–2425. [CrossRef]
83. Rousselot, I.; Taviot-Guého, C.; Besse, J.P. Synthesis and characterization of mixed Ga/Al-containing layered double hydroxides: Study of their basic properties through the Knoevenagel condensation of benzaldehyde and ethyl cyanoacetate, and comparison to other LDHs. *Int. J. Inorg. Mater.* **1999**, *1*, 165–174. [CrossRef]
84. Choudary, B.M.; Lakshmi Kantam, M.; Neeraja, V.; Koteswara Rao, K.; Figueras, F.; Delmotte, L. Layered double hydroxide fluoride: A novel solid base catalyst for C-C bond formation. *Green Chem.* **2001**, *3*, 257–260. [CrossRef]
85. Costantino, U.; Curini, M.; Montanari, F.; Nocchetti, M.; Rosati, O. Hydrotalcite-like compounds as catalysts in liquid phase organic synthesis I. Knoevenagel condensation promoted by $[Ni_{0.73}Al_{0.27}(OH)_2]$ $(CO_3)_{0.135}$. *J. Mol. Catal. A Chem.* **2003**, *195*, 245–252. [CrossRef]
86. Li, F.; Jiang, X.; Evans, D.G.; Duan, X. Structure and basicity of mesoporous materials from Mg/Al/In layered double hydroxides prepared by separate nucleation and aging steps method. *J. Porous Mater.* **2005**, *12*, 55–63. [CrossRef]
87. Lei, X.; Zhang, F.; Yang, L.; Guo, X.; Tian, Y.; Fu, S.; Li, F.; Evans, D.G.; Duan, X. Highly crystalline activated layered double hydroxides as solid acid-base catalysts. *AIChE J.* **2007**, *53*, 932–940. [CrossRef]
88. Jia, H.; Zhao, Y.; Niu, P.; Lu, N.; Fan, B.; Li, R. Amine-functionalized MgAl LDH nanosheets as efficient solid base catalysts for Knoevenagel condensation. *Mol. Catal.* **2018**, *449*, 31–37. [CrossRef]
89. Khan, F.A.; Dash, J.; Satapathy, R.; Upadhyay, S.K. Hydrotalcite catalysis in ionic liquid medium: A recyclable reaction system for heterogeneous Knoevenagel and nitroaldol condensation. *Tetrahedron Lett.* **2004**, *45*, 3055–3058. [CrossRef]
90. Li, T.; Zhang, W.; Chen, W.; Miras, H.N.; Song, Y.F. Layered double hydroxide anchored ionic liquids as amphiphilic heterogeneous catalysts for the Knoevenagel condensation reaction. *Dalt. Trans.* **2018**, *47*, 3059–3067. [CrossRef]
91. Zhou, W.; Zhai, S.; Pan, J.; Cui, A.; Qian, J.; He, M.; Xu, Z.; Chen, Q. Bifunctional NiGa Layered Double Hydroxide for the Aerobic Oxidation/Condensation Tandem Reaction between Aromatic Alcohols and Active Methylene Compounds. *Asian J. Org. Chem.* **2017**, *6*, 1536–1541. [CrossRef]
92. Bergmann, E.D.; Ginsburg, D.; Pappo, R. The Michael Reaction. In *Organic Reactions*; Major Reference Works; John Wiley & Sons, Inc.: New York, NY, USA, 2011; pp. 179–270. ISBN 9780471264187.
93. Michael, A. Ueber die Addition von Natriumacetessig- und Natriummalonsaureathern zu den Aethern ungesattigter Sauren. *J. Prakt. Chem.* **1887**, *35*, 349–356. [CrossRef]
94. Mather, B.D.; Viswanathan, K.; Miller, K.M.; Long, T.E. Michael addition reactions in macromolecular design for emerging technologies. *Prog. Polym. Sci.* **2006**, *31*, 487–531. [CrossRef]
95. Noomen, A. Applications of Michael addition chemistry in coatings technology. *Prog. Org. Coat.* **1997**, *32*, 137–142. [CrossRef]
96. Choudary, B.M.; Lakshmi Kantam, M.; Venkat Reddy, C.R.; Koteswara Rao, K.; Figueras, F. The first example of Michael addition catalysed by modified Mg-Al hydrotalcite. *J. Mol. Catal. A Chem.* **1999**, *146*, 279–284. [CrossRef]
97. Choudary, B.M.; Lakshmi Kantam, M.; Kavita, B.; Venkat Reddy, C.; Figueras, F. Catalytic C-C bond formation promoted by Mg-Al-O-t-Bu hydrotalcite. *Tetrahedron* **2000**, *56*, 9357–9364. [CrossRef]
98. Naciuk, F.F.; Vargas, D.Z.; D'oca, C.R.M.; Moro, C.C.; Russowsky, D. One pot domino reaction accessing γ-nitroesters: Synthesis of GABA derivatives. *New J. Chem.* **2015**, *39*, 1643–1653. [CrossRef]
99. Prescott, H.A.; Li, Z.J.; Kemnitz, E.; Trunschke, A.; Deutsch, J.; Lieske, H.; Auroux, A. Application of calcined Mg-Al hydrotalcites for Michael additions: An investigation of catalytic activity and acid-base properties. *J. Catal.* **2005**, *234*, 119–130. [CrossRef]

100. Ebitani, K.; Motokura, K.; Mori, K.; Mizugaki, T.; Kaneda, K. Reconstructed hydrotalcite as a highly active heterogeneous base catalyst for carbon-carbon bond formations in the presence of water. *J. Org. Chem.* **2006**, *71*, 5440–5447. [CrossRef]
101. Kantam, M.L.; Neelima, B.; Reddy, C.V. A recyclable protocol for aza-Michael addition of amines to α,β-unsaturated compounds using Cu-Al hydrotalcite. *J. Mol. Catal. A Chem.* **2005**, *241*, 147–150. [CrossRef]
102. Vijaikumar, S.; Dhakshinamoorthy, A.; Pitchumani, K. l-Proline anchored hydrotalcite clays: An efficient catalyst for asymmetric Michael addition. *Appl. Catal. A Gen.* **2008**, *340*, 25–32. [CrossRef]
103. Otera, J. Transesterification. *Chem. Rev.* **1993**, *93*, 1449–1470. [CrossRef]
104. Porter, R.S.; Wang, L.H. Compatibility and transesterification in binary polymer blends. *Polymer* **1992**, *33*, 2019–2030. [CrossRef]
105. Petrovic, Z.S. Polyurethanes from vegetable oils. *Polym. Rev.* **2008**, *48*, 109–155. [CrossRef]
106. Ma, F.; Hanna, M.A. Biodiesel production: A review. *Bioresour. Technol.* **2003**, *70*, 1–15. [CrossRef]
107. Cantrell, D.G.; Gillie, L.J.; Lee, A.F.; Wilson, K. Structure-reactivity correlations in MgAl hydrotalcite catalysts for biodiesel synthesis. *Appl. Catal. A Gen.* **2005**, *287*, 183–190. [CrossRef]
108. Zeng, H.Y.; Feng, Z.; Deng, X.; Li, Y.Q. Activation of Mg-Al hydrotalcite catalysts for transesterification of rape oil. *Fuel* **2008**, *87*, 3071–3076. [CrossRef]
109. Xie, W.; Peng, H.; Chen, L. Calcined Mg-Al hydrotalcites as solid base catalysts for methanolysis of soybean oil. *J. Mol. Catal. A Chem.* **2006**, *246*, 24–32. [CrossRef]
110. Liu, Y.; Lotero, E.; Goodwin, J.G.; Mo, X. Transesterification of poultry fat with methanol using Mg-Al hydrotalcite derived catalysts. *Appl. Catal. A Gen.* **2007**, *331*, 138–148. [CrossRef]
111. Navajas, A.; Campo, I.; Moral, A.; Echave, J.; Sanz, O.; Montes, M.; Odriozola, J.A.; Arzamendi, G.; Gandía, L.M. Outstanding performance of rehydrated Mg-Al hydrotalcites as heterogeneous methanolysis catalysts for the synthesis of biodiesel. *Fuel* **2018**, *211*, 173–181. [CrossRef]
112. Kondawar, S.; Rode, C. Solvent-Free Glycerol Transesterification with Propylene Carbonate to Glycerol Carbonate over a Solid Base Catalyst. *Energy Fuels* **2017**, *31*, 4361–4371. [CrossRef]
113. Yagiz, F.; Kazan, D.; Akin, A.N. Biodiesel production from waste oils by using lipase immobilized on hydrotalcite and zeolites. *Chem. Eng. J.* **2007**, *134*, 262–267. [CrossRef]
114. Giannelis, E.P.; Nocera, D.G.; Pinnavaia, T.J. Anionic Photocatalysts Supported in Layered Double Hydroxides: Intercalation and Photophysical Properties of a Ruthenium Complex Anion in Synthetic Hydrotalcite. *Inorg. Chem.* **1987**, *26*, 203–205. [CrossRef]
115. Kwon, T.; Tsigdinos, G.A.; Pinnavaia, T.J. Pillaring of Layered Double Hydroxides (LDH's) by Polyoxometalate Anions. *J. Am. Chem. Soc.* **1988**, *110*, 3653–3654. [CrossRef]
116. Seftel, E.M.; Popovici, E.N.; Mertens, M.; Stefaniak, E.A.; Van Grieken, R.; Cool, P.; Vansant, E.F. SnIV-containing layered double hydroxides as precursors for nano-sized ZnO/SnO_2 photocatalysts. *Appl. Catal. B Environ.* **2008**, *84*, 699–705. [CrossRef]
117. Seftel, E.M.; Popovici, E.N.; Mertens, M.; De Witte, K.; Van Tendeloo, G.; Cool, P.; Vansant, E.F. Zn-Al layered double hydroxides: Synthesis, characterization and photocatalytic application. *Microporous Mesoporous Mater.* **2008**, *113*, 296–304. [CrossRef]
118. Jingshan, L.; Jeong-Hyeok, I.; Mayer, M.T.; Marcel, S.; Mohammad Khaja, N.; Nam-Gyu, P.; S David, T.; Jin, F.H.; Michael, G. Water photolysis at 12.3% efficiency via perovskite photovoltaics and Earth-abundant catalysts. *Science* **2014**, *345*, 1593–1596.
119. Mohapatra, L.; Parida, K. A review on the recent progress, challenges and perspective of layered double hydroxides as promising photocatalysts. *J. Mater. Chem. A* **2016**, *4*, 10744–10766. [CrossRef]
120. Greene, J.C.; Baughman, G.L. Effects of 46 Dyes on Population Growth of Freshwater Green Alga Se/eksfrum capricornutum. *Text. Chem. Color.* **1996**, *28*, 23–30.
121. Gregory, P. 3—Toxicology of textile dyes. In *Woodhead Publishing Series in Textiles*; Christie, R.M., Ed.; Woodhead Publishing: Cambridge, UK, 2007; pp. 44–73. ISBN 978-1-84569-115-8.
122. Hatch, K.L.; Maibach, H. Dyes as Contact Allergens: A Comprehensive Record. *Text. Chem. Color. Am. Dyest. Report.* **1999**, *1*, 53–59.
123. Kuo, W.G. Decolorizing dye wastewater with Fenton's reagent. *Water Res.* **1992**, *26*, 881–886. [CrossRef]
124. Rai, H.S.; Bhattacharyya, M.S.; Singh, J.; Bansal, T.K.; Vats, P.; Banerjee, U.C. Removal of dyes from the effluent of textile and dyestuff manufacturing industry: A review of emerging techniques with reference to biological treatment. *Crit. Rev. Environ. Sci. Technol.* **2005**, *35*, 219–238. [CrossRef]

125. Gupta, V.K. Suhas Application of low-cost adsorbents for dye removal—A review. *J. Environ. Manage.* **2009**, *90*, 2313–2342. [CrossRef]
126. Seftel, E.M.; Popovici, E.N.; Beyers, E.; Mertens, M.; Zhu, H.; Vansant, E.F.; Cool, P. New TiO_2/MgAl-LDH Nanocomposites for the Photocatalytic Degradation of Dyes. *J. Nanosci. Nanotechnol.* **2010**, *10*, 8227–8233. [CrossRef] [PubMed]
127. Parida, K.; Mohapatra, L. Carbonate intercalated Zn/Fe layered double hydroxide: A novel photocatalyst for the enhanced photo degradation of azo dyes. *Chem. Eng. J.* **2012**, *179*, 131–139. [CrossRef]
128. Abderrazek, K.; Najoua, F.S.; Srasra, E. Synthesis and characterization of [Zn-Al] LDH: Study of the effect of calcination on the photocatalytic activity. *Appl. Clay Sci.* **2016**, *119*, 229–235. [CrossRef]
129. Ao, Y.; Wang, D.; Wang, P.; Wang, C.; Hou, J.; Qian, J. Enhanced photocatalytic properties of the 3D flower-like Mg-Al layered double hydroxides decorated with Ag_2CO_3 under visible light illumination. *Mater. Res. Bull.* **2016**, *80*, 23–29. [CrossRef]
130. Dinari, M.; Momeni, M.M.; Ghayeb, Y. Photodegradation of organic dye by ZnCrLa-layered double hydroxide as visible-light photocatalysts. *J. Mater. Sci. Mater. Electron.* **2016**, *27*, 9861–9869. [CrossRef]
131. Suárez-Quezada, M.; Romero-Ortiz, G.; Suárez, V.; Morales-Mendoza, G.; Lartundo-Rojas, L.; Navarro-Cerón, E.; Tzompantzi, F.; Robles, S.; Gómez, R.; Mantilla, A. Photodegradation of phenol using reconstructed Ce doped Zn/Al layered double hydroxides as photocatalysts. *Catal. Today* **2016**, *271*, 213–219. [CrossRef]
132. Wu, X.; Zhang, D.; Jiao, F.; Wang, S. Visible-light-driven photodegradation of Methyl Orange using Cu_2O/ZnAl calcined layered double hydroxides as photocatalysts. *Colloids Surf. A Physicochem. Eng. Asp.* **2016**, *508*, 110–116. [CrossRef]
133. Carja, G.; Grosu, E.F.; Mureseanu, M.; Lutic, D. A family of solar light responsive photocatalysts obtained using Zn^{2+} Me^{3+} (Me = Al/Ga) LDHs doped with Ga_2O_3 and In_2O_3 and their derived mixed oxides: A case study of phenol/4-nitrophenol decomposition. *Catal. Sci. Technol.* **2017**, *7*, 5402–5412. [CrossRef]
134. Hadnadjev-Kostic, M.; Vulic, T.; Marinkovic-Neducin, R.; Lončarević, D.; Dostanić, J.; Markov, S.; Jovanović, D. Photo-induced properties of photocatalysts: A study on the modified structural, optical and textural properties of TiO_2–ZnAl layered double hydroxide based materials. *J. Clean. Prod.* **2017**, *164*, 1–18. [CrossRef]
135. Mohamed, F.; Abukhadra, M.R.; Shaban, M. Removal of safranin dye from water using polypyrrole nanofiber/Zn-Fe layered double hydroxide nanocomposite (Ppy NF/Zn-Fe LDH) of enhanced adsorption and photocatalytic properties. *Sci. Total Environ.* **2018**, *640–641*, 352–363. [CrossRef] [PubMed]
136. Timár, Z.; Varga, G.; Muráth, S.; Kónya, Z.; Kukovecz, Á. Synthesis, characterization and photocatalytic activity of crystalline Mn (II) Cr (III) -layered double hydroxide. *Catal. Today* **2017**, *284*, 195–201. [CrossRef]
137. Fu, Y.; Ning, F.; Xu, S.; An, H.; Shao, M.; Wei, M. Terbium doped ZnCr-layered double hydroxides with largely enhanced visible light photocatalytic performance. *J. Mater. Chem. A* **2016**, *4*, 3907–3913. [CrossRef]
138. Silva, C.G.; Bouizi, Y.; Fornés, V.; García, H. Layered double hydroxides as highly efficient photocatalysts for visible light oxygen generation from water. *J. Am. Chem. Soc.* **2009**, *131*, 13833–13839. [CrossRef] [PubMed]
139. Lee, J.M.; Yang, J.H.; Kwon, N.H.; Jo, Y.K.; Choy, J.H.; Hwang, S.J. Intercalative hybridization of layered double hydroxide nanocrystals with mesoporous g-C_3N_4 for enhancing visible light-induced H_2 production efficiency. *Dalt. Trans.* **2018**, *47*, 2949–2955. [CrossRef] [PubMed]
140. Wang, R.; Luo, L.; Zhu, X.; Yan, Y.; Zhang, B.; Xiang, X.; He, J. Plasmon-Enhanced Layered Double Hydroxide Composite $BiVO_4$ Photoanodes: Layering-Dependent Modulation of the Water-Oxidation Reaction. *ACS Appl. Energy Mater.* **2018**, *1*, 3577–3586. [CrossRef]
141. Vo, T.G.; Tai, Y.; Chiang, C.Y. Multifunctional ternary hydrotalcite-like nanosheet arrays as an efficient co-catalyst for vastly improved water splitting performance on bismuth vanadate photoanode. *J. Catal.* **2019**, *370*, 1–10. [CrossRef]
142. Ma, Y.; Wang, X.; Jia, Y.; Chen, X.; Han, H.; Li, C. Titanium Dioxide-Based Nanomaterials for Photocatalytic Fuel Generations. *Chem. Rev.* **2014**, *114*, 9987–10043. [CrossRef]
143. Tu, W.; Zhou, Y.; Zou, Z. Photocatalytic conversion of CO_2 into renewable hydrocarbon fuels: State-of-the-art accomplishment, challenges, and prospects. *Adv. Mater.* **2014**, *26*, 4607–4626. [CrossRef]
144. White, J.L.; Baruch, M.F.; Pander, J.E.; Hu, Y.; Fortmeyer, I.C.; Park, J.E.; Zhang, T.; Liao, K.; Gu, J.; Yan, Y.; et al. Light-Driven Heterogeneous Reduction of Carbon Dioxide: Photocatalysts and Photoelectrodes. *Chem. Rev.* **2015**, *115*, 12888–12935. [CrossRef]

145. Sharma, U.; Tyagi, B.; Jasra, R.V. Synthesis and Characterization of Mg-Al-CO_3 Layered Double Hydroxide for CO_2 Adsorption. *Ind. Eng. Chem. Res.* **2008**, *47*, 9588–9595. [CrossRef]
146. Flores-Flores, M.; Luévano-Hipólito, E.; Martínez, L.M.T.; Morales-Mendoza, G.; Gómez, R. Photocatalytic CO_2 conversion by MgAl layered double hydroxides: Effect of Mg^{2+} precursor and microwave irradiation time. *J. Photochem. Photobiol. A Chem.* **2018**, *363*, 68–73. [CrossRef]
147. Iguchi, S.; Teramura, K.; Hosokawa, S.; Tanaka, T. Photocatalytic conversion of CO_2 in water using fluorinated layered double hydroxides as photocatalysts. *Appl. Catal. A Gen.* **2016**, *521*, 160–167. [CrossRef]
148. Anton Wein, L.; Zhang, H.; Urushidate, K.; Miyano, M.; Izumi, Y. Optimized photoreduction of CO_2 exclusively into methanol utilizing liberated reaction space in layered double hydroxides comprising zinc, copper, and gallium. *Appl. Surf. Sci.* **2018**, *447*, 687–696. [CrossRef]
149. Iguchi, S.; Hasegawa, Y.; Teramura, K.; Hosokawa, S.; Tanaka, T. Preparation of transition metal-containing layered double hydroxides and application to the photocatalytic conversion of CO_2 in water. *J. CO2 Util.* **2016**, *15*, 6–14. [CrossRef]
150. Tokudome, Y.; Fukui, M.; Iguchi, S.; Hasegawa, Y.; Teramura, K.; Tanaka, T.; Takemoto, M.; Katsura, R.; Takahashi, M. A nanoLDH catalyst with high CO_2 adsorption capability for photo-catalytic reduction. *J. Mater. Chem. A* **2018**, *6*, 9684–9690. [CrossRef]
151. Zhao, H.; Xu, J.; Liu, L.; Rao, G.; Zhao, C.; Li, Y. CO_2 photoreduction with water vapor by Ti-embedded MgAl layered double hydroxides. *J. CO2 Util.* **2016**, *15*, 15–23. [CrossRef]
152. Tonda, S.; Kumar, S.; Bhardwaj, M.; Yadav, P.; Ogale, S. g-C_3N_4/NiAl-LDH 2D/2D Hybrid Heterojunction for High-Performance Photocatalytic Reduction of CO_2 into Renewable Fuels. *ACS Appl. Mater. Interfaces* **2018**, *10*, 2667–2678. [CrossRef]
153. Gao, L.G.; Gao, Y.Y.; Song, X.L.; Ma, X. rong A novel La^{3+}–Zn^{2+}–Al^{3+}–MoO_4^{2-} layered double hydroxides photocatalyst for the decomposition of dibenzothiophene in diesel oil. *Pet. Sci. Technol.* **2018**, *36*, 850–855. [CrossRef]
154. Ristovski, Z.D.; Jayaratne, R.E.; Lim, M.; Ayoko, G.A.; Morawska, L. Influence of diesel fuel sulfur on nanoparticle emissions from city buses. *Environ. Sci. Technol.* **2006**, *40*, 1314–1320. [CrossRef]
155. Postgate, J.R. Biological nitrogen fixation: Fundamentals. *Philos. Trans. R. Soc. Lond. B. Biol. Sci.* **1982**, *296*, 375–385. [CrossRef]
156. Appl, M. Chemical Reactions and Uses of Ammonia. In *Ammonia: Principles and Industrial Practice*; Wiley Online Books: New York, NY, USA, 1999; pp. 231–234. ISBN 9783527613885. Available online: https://onlinelibrary.wiley.com/doi/book/10.1002/9783527613885 (accessed on 3 June 2019).
157. Erisman, J.W.; Sutton, M.A.; Galloway, J.; Klimont, Z.; Winiwarter, W. How a century of ammonia synthesis changed the world. *Nat. Geosci.* **2008**, *1*, 636–639. [CrossRef]
158. Zhao, Y.; Zhao, Y.; Waterhouse, G.I.N.; Zheng, L.; Cao, X.; Teng, F.; Wu, L.; Tung, C.; Hare, D.O.; Zhang, T. Layered-Double-Hydroxide Nanosheets as Efficient Visible-Light-Driven Photocatalysts for Dinitrogen Fixation. *Adv. Mater.* **2017**, *29*, 1703828. [CrossRef] [PubMed]
159. Cnrs, U.M.R.; Lyon, E.C. De Urea Biosensors Based on Immobilization of Urease into Two Oppositely Charged Clays (Laponite and Zn-Al Layered Double Hydroxides) the effect of the buffer capacity of the outer medium. *Anal. Chem.* **2002**, *74*, 4037–4043.
160. Taviot-Guého, C.; Prévot, V.; Forano, C.; Renaudin, G.; Mousty, C.; Leroux, F. Tailoring Hybrid Layered Double Hydroxides for the Development of Innovative Applications. *Adv. Funct. Mater.* **2018**, *28*, 1703868. [CrossRef]
161. Wang, J. Electrochemical Glucose Biosensors. *Chem. Rev.* **2008**, *108*, 814–825. [CrossRef] [PubMed]
162. Aleeva, Y.; Maira, G.; Scopelliti, M.; Vinciguerra, V.; Scandurra, G.; Cannatà, G.; Giusi, G.; Ciofi, C.; Figà, V.; Occhipinti, L.G.; et al. Amperometric Biosensor and Front-End Electronics for Remote Glucose Monitoring by Crosslinked PEDOT-Glucose Oxidase. *IEEE Sens. J.* **2018**, *18*, 4869–4878. [CrossRef]
163. Toghill, K.E.; Compton, R.G. Electrochemical Non-enzymatic Glucose Sensors: A Perspective and an Evaluation. *Int. J. Electrochem. Sci* **2010**, *5*, 1246–1301.
164. Cui, J.; Li, Z.; Liu, K.; Li, J.; Shao, M. A bifunctional nonenzymatic flexible glucose microsensor based on CoFe-Layered double hydroxide. *Nanoscale Adv.* **2019**, *1*, 948–952. [CrossRef]
165. Ai, H.; Huang, X.; Zhu, Z.; Liu, J.; Chi, Q.; Li, Y.; Li, Z.; Ji, X. A novel glucose sensor based on monodispersed Ni/Al layered double hydroxide and chitosan. *Biosens. Bioelectron.* **2008**, *24*, 1048–1052. [CrossRef]

166. Li, X.; Liu, J.; Ji, X.; Jiang, J.; Ding, R.; Hu, Y.; Hu, A.; Huang, X. Ni/Al layered double hydroxide nanosheet film grown directly on Ti substrate and its application for a nonenzymatic glucose sensor. *Sens. Actuators B Chem.* **2010**, *147*, 241–247. [CrossRef]
167. Fu, S.; Fan, G.; Yang, L.; Li, F. Non-enzymatic glucose sensor based on Au nanoparticles decorated ternary Ni-Al layered double hydroxide/single-walled carbon nanotubes/graphene nanocomposite. *Electrochim. Acta* **2015**, *152*, 146–154. [CrossRef]
168. Hassanein, A.; Salahuddin, N.; Matsuda, A.; Hattori, T.; Elfiky, M. Fabrication of Electrochemical Sensor Based on Layered Double Hydroxide/Polypyrrole/Carbon Paste for Determination of an Alpha-adrenergic Blocking Agent Terazosin. *Electroanalysis* **2018**, *30*, 459–465. [CrossRef]
169. Ma, Y.; Wang, Y.; Xie, D.; Gu, Y.; Zhang, H.; Wang, G.; Zhang, Y.; Zhao, H.; Wong, P.K. NiFe-Layered Double Hydroxide Nanosheet Arrays Supported on Carbon Cloth for Highly Sensitive Detection of Nitrite. *ACS Appl. Mater. Interfaces* **2018**, *10*, 6541–6551. [CrossRef] [PubMed]
170. Asif, M.; Aziz, A.; Wang, H.; Wang, Z.; Wang, W.; Ajmal, M.; Xiao, F.; Chen, X.; Liu, H. Superlattice stacking by hybridizing layered double hydroxide nanosheets with layers of reduced graphene oxide for electrochemical simultaneous determination of dopamine, uric acid and ascorbic acid. *Microchim. Acta* **2019**, *186*, 61. [CrossRef] [PubMed]
171. Liu, J.; Xu, X.; Chen, Z.; Li, R.; Kang, L.; Yao, J. A fluorometric displacement assay for adenosine triphosphate using layered cobalt(II) double hydroxide nanosheets. *Microchim. Acta* **2019**, *186*, 263. [CrossRef] [PubMed]
172. Abdolmohammad-Zadeh, H.; Zamani-Kalajahi, M. A turn-on/off fluorescent sensor based on nano-structured Mg-Al layered double hydroxide intercalated with salicylic acid for monitoring of ferric ion in human serum samples. *Anal. Chim. Acta* **2019**, *1061*, 152–160. [CrossRef] [PubMed]
173. Arrabito, G.; Galati, C.; Castellano, S.; Pignataro, B. Luminometric sub-nanoliter droplet-to-droplet array (LUMDA) and its application to drug screening by phase I metabolism enzymes. *Lab Chip* **2013**, *13*, 68–72. [CrossRef] [PubMed]
174. Wang, Z.; Liu, F.; Lu, C. Chemiluminescence flow biosensor for glucose using Mg-Al carbonate layered double hydroxides as catalysts and buffer solutions. *Biosens. Bioelectron.* **2012**, *38*, 284–288. [CrossRef]
175. Pourfaraj, R.; Kazemi, S.Y.; Fatemi, S.J.; Biparva, P. Synthesis of α- and β-CoNi binary hydroxides nanostructures and luminol chemiluminescence study for H_2O_2 detection. *J. Photochem. Photobiol. A Chem.* **2018**, *364*, 534–541. [CrossRef]
176. Pan, F.; Zhang, Y.; Yuan, Z.; Lu, C. Sensitive and Selective Carmine Acid Detection Based on Chemiluminescence Quenching of Layer Doubled Hydroxide–Luminol–H_2O_2 System. *ACS Omega* **2018**, *3*, 18836–18842. [CrossRef]
177. Haroone, M.S.; Hu, Y.; Zhang, P.; Ma, R.; Zhang, X.; Kaleem, Q.M.; Khan, M.B.; Lu, J. Fluorescence enhancement strategy for evaluation of the minor groove binder DAPI to complementary ssDNA sequence including telomere mimics in $(ssDNA@DAPI/LDH)_n$ ultrathin films. *Dyes Pigments* **2019**, *166*, 422–432. [CrossRef]
178. Fu, L.; Yan, L.; Wang, G.; Ren, H.; Jin, L. Photoluminescence enhancement of silver nanoclusters assembled on the layered double hydroxides and their application to guanine detection. *Talanta* **2019**, *193*, 161–167. [CrossRef] [PubMed]
179. Aziz, A.; Asif, M.; Azeem, M.; Ashraf, G.; Wang, Z.; Xiao, F.; Liu, H. Self-stacking of exfoliated charged nanosheets of LDHs and graphene as biosensor with real-time tracking of dopamine from live cells. *Anal. Chim. Acta* **2019**, *1047*, 197–207. [CrossRef] [PubMed]
180. Asif, M.; Aziz, A.; Wang, Z.; Ashraf, G.; Wang, J.; Luo, H.; Chen, X.; Xiao, F.; Liu, H. Hierarchical CNTs@CuMn layered double hydroxide nanohybrid with enhanced electrochemical performance in H_2S detection from live cells. *Anal. Chem.* **2019**, *91*, 3912–3920. [CrossRef]
181. Chatterjee, A.; Bharadiya, P.; Hansora, D. Layered double hydroxide based bionanocomposites. *Appl. Clay Sci.* **2019**, *177*, 19–36. [CrossRef]
182. Andrea, K.A.; Wang, L.; Carrier, A.J.; Campbell, M.; Buhariwalla, M.; Mutch, M.; MacQuarrie, S.L.; Bennett, C.; Mkandawire, M.; Oakes, K.; et al. Adsorption of Oligo-DNA on Magnesium Aluminum-Layered Double-Hydroxide Nanoparticle Surfaces: Mechanistic Implication in Gene Delivery. *Langmuir* **2017**, *33*, 3926–3933. [CrossRef] [PubMed]

183. Lu, M.; Shan, Z.; Andrea, K.; Macdonald, B.; Beale, S.; Curry, D.E.; Wang, L.; Wang, S.; Oakes, K.D.; Bennett, C.; et al. Chemisorption Mechanism of DNA on Mg/Fe Layered Double Hydroxide Nanoparticles: Insights into Engineering Effective SiRNA Delivery Systems. *Langmuir* **2016**, *32*, 2659–2667. [CrossRef] [PubMed]
184. Choy, J.-H.; Kwak, S.-Y.; Park, J.-S.; Jeong, Y.-J.; Portier, J. Intercalative Nanohybrids of Nucleoside Monophosphates and DNA in Layered Metal Hydroxide. *J. Am. Chem. Soc.* **1999**, *121*, 1399–1400. [CrossRef]
185. Desigaux, L.; Belkacem, M.B.; Richard, P.; Cellier, J.; Léone, P.; Cario, L.; Leroux, F.; Taviot-Guého, C.; Pitard, B. Self-assembly and characterization of layered double hydroxide/DNA hybrids. *Nano Lett.* **2006**, *6*, 199–204. [CrossRef] [PubMed]
186. Choy, J.-H.; Kwak, S.-Y.; Jeong, Y.-J.; Park, J.-S. Inorganic Layered Double Hydroxides as Nonviral Vectors. *Angew. Chem. Int. Ed.* **2000**, *39*, 4041–4045. [CrossRef]
187. Yazdani, P.; Mansouri, E.; Eyvazi, S.; Yousefi, V.; Kahroba, H.; Hejazi, M.S.; Mesbahi, A.; Tarhriz, V.; Abolghasemi, M.M. Layered double hydroxide nanoparticles as an appealing nanoparticle in gene/plasmid and drug delivery system in C2C12 myoblast cells. *Artif. Cells Nanomed. Biotechnol.* **2019**, *47*, 436–442. [CrossRef] [PubMed]
188. Li, Y.; Bao, W.; Wu, H.; Wang, J.; Zhang, Y.; Wan, Y.; Cao, D.; O'Hare, D.; Wang, Q. Delaminated layered double hydroxide delivers DNA molecules as sandwich nanostructure into cells via a non-endocytic pathway. *Sci. Bull.* **2017**, *62*, 686–692. [CrossRef]
189. Ádok-Sipiczki, M.; Szilagyi, I.; Pálinkó, I.; Pavlovic, M.; Sipos, P.; Nardin, C. Design of nucleic acid-layered double hydroxide nanohybrids. *Colloid Polym. Sci.* **2017**, *295*, 1463–1473. [CrossRef]
190. Wong, Y.; Markham, K.; Xu, Z.P.; Chen, M.; Max Lu, G.Q.; Bartlett, P.F.; Cooper, H.M. Efficient delivery of siRNA to cortical neurons using layered double hydroxide nanoparticles. *Biomaterials* **2010**, *31*, 8770–8779. [CrossRef]
191. Li, L.; Gu, W.; Chen, J.; Chen, W.; Xu, Z.P. Co-delivery of siRNAs and anti-cancer drugs using layered double hydroxide nanoparticles. *Biomaterials* **2014**, *35*, 3331–3339. [CrossRef]
192. Park, D.H.; Cho, J.; Kwon, O.J.; Yun, C.O.; Choy, J.H. Biodegradable Inorganic Nanovector: Passive versus Active Tumor Targeting in siRNA Transportation. *Angew. Chem. Int. Ed.* **2016**, *55*, 4582–4586. [CrossRef]
193. Acharya, R.; Alsharabasy, A.M.; Saha, S.; Rahaman, S.H.; Bhattacharjee, A.; Halder, S.; Chakraborty, M.; Chakraborty, J. Intercalation of shRNA-plasmid in Mg–Al layered double hydroxide nanoparticles and its cellular internalization for possible treatment of neurodegenerative diseases. *J. Drug Deliv. Sci. Technol.* **2019**, *52*, 500–508. [CrossRef]
194. Rahaman, S.H.; Bhattacharjee, A.; Saha, S.; Chakraborty, M.; Chakraborty, J. shRNA intercalation in CaAl-LDH nanoparticle synthesized at two different pH conditions and its comparative evaluation. *Appl. Clay Sci.* **2019**, *171*, 57–64. [CrossRef]
195. Li, L.; Zhang, R.; Gu, W.; Xu, Z.P. Mannose-conjugated layered double hydroxide nanocomposite for targeted siRNA delivery to enhance cancer therapy. *Nanomed. Nanotechnol. Biol. Med.* **2018**, *14*, 2355–2364. [CrossRef]
196. Wu, Y.; Gu, W.; Li, L.; Chen, C.; Xu, Z. Enhancing PD-1 Gene Silence in T Lymphocytes by Comparing the Delivery Performance of Two Inorganic Nanoparticle Platforms. *Nanomaterials* **2019**, *9*, 159. [CrossRef]
197. Wu, Y.; Gu, W.; Chen, C.; Do, S.T.; Xu, Z.P. Optimization of Formulations Consisting of Layered Double Hydroxide Nanoparticles and Small Interfering RNA for Efficient Knockdown of the Target Gene. *ACS Omega* **2018**, *3*, 4871–4877. [CrossRef] [PubMed]
198. Santos, A.C.; Ferreira, C.; Veiga, F.; Ribeiro, A.J.; Panchal, A.; Lvov, Y.; Agarwal, A. Halloysite clay nanotubes for life sciences applications: From drug encapsulation to bioscaffold. *Adv. Colloid Interface Sci.* **2018**, *257*, 58–70. [CrossRef] [PubMed]
199. Massaro, M.; Cavallaro, G.; Colletti, C.G.; Lazzara, G.; Milioto, S.; Noto, R.; Riela, S. Chemical modification of halloysite nanotubes for controlled loading and release. *J. Mater. Chem. B* **2018**, *6*, 3415–3433. [CrossRef]
200. Arrabito, G.; Cavaleri, F.; Montalbano, V.; Vetri, V.; Leone, M.; Pignataro, B. Monitoring few molecular binding events in scalable confined aqueous compartments by raster image correlation spectroscopy (CADRICS). *Lab Chip* **2016**, *16*, 4666–4676. [CrossRef] [PubMed]
201. Kumar, B.V.V.S.P.; Patil, A.J.; Mann, S. Enzyme-powered motility in buoyant organoclay/DNA protocells. *Nat. Chem.* **2018**, *10*, 1154–1163. [CrossRef] [PubMed]
202. Choi, G.; Eom, S.; Vinu, A.; Choy, J.H. 2D Nanostructured Metal Hydroxides with Gene Delivery and Theranostic Functions; A Comprehensive Review. *Chem. Rec.* **2018**, *18*, 1033–1053. [CrossRef] [PubMed]

203. Forano, C.; Bruna, F.; Mousty, C.; Prevot, V. Interactions between Biological Cells and Layered Double Hydroxides: Towards Functional Materials. *Chem. Rec.* **2018**, *18*, 1150–1166. [CrossRef]
204. Kura, A.U.; Hussein, M.Z.; Fakurazi, S.; Arulselvan, P. Layered double hydroxide nanocomposite for drug delivery systems; bio-distribution, toxicity and drug activity enhancement. *Chem. Cent. J.* **2014**, *8*, 47. [CrossRef]
205. Choi, S.-J.; Choy, J.-H. Layered double hydroxide nanoparticles as target-specific delivery carriers: Uptake mechanism and toxicity. *Nanomedicine* **2011**, *6*, 803–814. [CrossRef]
206. Saifullah, B.; Hussein, M.Z.; Hussein-Al-Ali, S.H.; Arulselvan, P.; Fakurazi, S. Antituberculosis nanodelivery system with controlled-release properties based on para-amino salicylate—Zinc aluminum-layered double-hydroxide nanocomposites. *Drug Des Devel Ther.* **2013**, *7*, 1365–1375.
207. da Costa Fernandes, C., Jr.; Pinto, T.S.; Kang, H.R.; Magalhães Padilha, P.; Koh, I.H.J.; Constantino, V.R.L.; Zambuzzi, W.F. Layered Double Hydroxides Are Promising Nanomaterials for Tissue Bioengineering Application. *Adv. Biosyst.* **2019**, 1800238. [CrossRef]
208. Cunha, V.R.R.; De Souza, R.B.; Da Fonseca Martins, A.M.C.R.P.; Koh, I.H.J.; Constantino, V.R.L. Accessing the biocompatibility of layered double hydroxide by intramuscular implantation: Histological and microcirculation evaluation. *Sci. Rep.* **2016**, *6*, 30547. [CrossRef] [PubMed]
209. Li, H.; Peng, F.; Wang, D.; Qiao, Y.; Xu, D.; Liu, X. Layered double hydroxide/poly-dopamine composite coating with surface heparinization on Mg alloys: Improved anticorrosion, endothelialization and hemocompatibility. *Biomater. Sci.* **2018**, *6*, 1846–1858. [CrossRef] [PubMed]
210. Peng, F.; Li, H.; Wang, D.; Tian, P.; Tian, Y.; Yuan, G.; Xu, D.; Liu, X. Enhanced Corrosion Resistance and Biocompatibility of Magnesium Alloy by Mg–Al-Layered Double Hydroxide. *ACS Appl. Mater. Interfaces* **2016**, *8*, 35033–35044. [CrossRef]
211. Errico, V.; Arrabito, G.; Fornetti, E.; Fuoco, C.; Testa, S.; Saggio, G.; Rufini, S.; Cannata, S.; Desideri, A.; Falconi, C.; et al. High-Density ZnO Nanowires as a Reversible Myogenic–Differentiation Switch. *ACS Appl. Mater. Interfaces* **2018**, *10*, 14097–14107. [CrossRef]
212. Hansel, C.S.; Crowder, S.W.; Cooper, S.; Gopal, S.; João Pardelha da Cruz, M.; de Oliveira Martins, L.; Keller, D.; Rothery, S.; Becce, M.; Cass, A.E.G.; et al. Nanoneedle-Mediated Stimulation of Cell Mechanotransduction Machinery. *ACS Nano* **2019**, *13*, 2913–2926. [CrossRef]
213. Ramanathan, G.; Liji, L.S.; Fardim, P.; Sivagnanam, U.T. Fabrication of 3D dual-layered nanofibrous graft loaded with layered double hydroxides and their effects in osteoblastic behavior for bone tissue engineering. *Process Biochem.* **2018**, *64*, 255–259. [CrossRef]
214. Lee, S.S.; Choi, G.E.; Lee, H.J.; Kim, Y.; Choy, J.H.; Jeong, B. Layered Double Hydroxide and Polypeptide Thermogel Nanocomposite System for Chondrogenic Differentiation of Stem Cells. *ACS Appl. Mater. Interfaces* **2017**, *9*, 42668–42675. [CrossRef]
215. Kang, H.R.; da Costa Fernandes, C.J.; da Silva, R.A.; Constantino, V.R.L.; Koh, I.H.J.; Zambuzzi, W.F. Mg–Al and Zn–Al Layered Double Hydroxides Promote Dynamic Expression of Marker Genes in Osteogenic Differentiation by Modulating Mitogen-Activated Protein Kinases. *Adv. Healthc. Mater.* **2018**, *7*, 1700693. [CrossRef]
216. da Silva Feltran, G.; da Costa Fernandes, C.J.; Rodrigues Ferreira, M.; Kang, H.R.; de Carvalho Bovolato, A.L.; de Assis Golim, M.; Deffune, E.; Koh, I.H.J.; Constantino, V.R.L.; Zambuzzi, W.F. Sonic hedgehog drives layered double hydroxides-induced acute inflammatory landscape. *Colloids Surf. B Biointerfaces* **2019**, *174*, 467–475. [CrossRef]
217. Li, B.; Gu, Z.; Kurniawan, N.; Chen, W.; Xu, Z.P. Manganese-Based Layered Double Hydroxide Nanoparticles as a T1-MRI Contrast Agent with Ultrasensitive pH Response and High Relaxivity. *Adv. Mater.* **2017**, *29*, 1700373. [CrossRef]
218. Saha, S.; Ray, S.; Acharya, R.; Chatterjee, T.K.; Chakraborty, J. Magnesium, zinc and calcium aluminium layered double hydroxide-drug nanohybrids: A comprehensive study. *Appl. Clay Sci.* **2017**, *135*, 493–509. [CrossRef]
219. Naz, S.; Shamoon, M.; Wang, R.; Zhang, L.; Zhou, J.; Chen, J. Advances in therapeutic implications of inorganic drug delivery nano-platforms for cancer. *Int. J. Mol. Sci.* **2019**, *20*, 965. [CrossRef]
220. Lv, F.; Xu, L.; Zhang, Y.; Meng, Z. Layered Double Hydroxide Assemblies with Controllable Drug Loading Capacity and Release Behavior as well as Stabilized Layer-by-Layer Polymer Multilayers. *ACS Appl. Mater. Interfaces* **2015**, *7*, 19104–19111. [CrossRef]

221. Choi, G.; Lee, J.H.; Oh, Y.J.; Choy, Y.B.; Park, M.C.; Chang, H.C.; Choy, J.H. Inorganic-polymer nanohybrid carrier for delivery of a poorly-soluble drug, ursodeoxycholic acid. *Int. J. Pharm.* **2010**, *402*, 117–122. [CrossRef]
222. Gu, Z.; Zuo, H.; Li, L.; Wu, A.; Xu, Z.P. Pre-coating layered double hydroxide nanoparticles with albumin to improve colloidal stability and cellular uptake. *J. Mater. Chem. B* **2015**, *3*, 3331–3339. [CrossRef]
223. Oh, J.-M.; Choi, S.-J.; Kim, S.-T.; Choy, J.-H. Cellular Uptake Mechanism of an Inorganic Nanovehicle and Its Drug Conjugates: Enhanced Efficacy Due To Clathrin-Mediated Endocytosis. *Bioconjug. Chem.* **2006**, *17*, 1411–1417. [CrossRef]
224. Bao, W.; Wang, J.; Wang, Q.; O'Hare, D.; Wan, Y. Layered double hydroxide nanotransporter for molecule delivery to intact plant cells. *Sci. Rep.* **2016**, *6*, 26738. [CrossRef]
225. Kong, X.; Jin, L.; Wei, M.; Duan, X. Antioxidant drugs intercalated into layered double hydroxide: Structure and in vitro release. *Appl. Clay Sci.* **2010**, *49*, 324–329. [CrossRef]
226. Rojas, R.; Palena, M.C.; Jimenez-Kairuz, A.F.; Manzo, R.H.; Giacomelli, C.E. Modeling drug release from a layered double hydroxide-ibuprofen complex. *Appl. Clay Sci.* **2012**, *62–63*, 15–20. [CrossRef]
227. Yasaei, M.; Khakbiz, M.; Ghasemi, E.; Zamanian, A. Synthesis and characterization of ZnAl-NO_3(CO_3) layered double hydroxide: A novel structure for intercalation and release of simvastatin. *Appl. Surf. Sci.* **2019**, *467–468*, 782–791. [CrossRef]
228. Bouaziz, Z.; Djebbi, M.A.; Soussan, L.; Janot, J.M.; Amara, A.B.H.; Balme, S. Adsorption of nisin into layered double hydroxide nanohybrids and in-vitro controlled release. *Mater. Sci. Eng. C* **2017**, *76*, 673–683. [CrossRef]
229. Mallakpour, S.; Hatami, M. Fabrication and characterization of pH-sensitive bio-nanocomposite beads havening folic acid intercalated LDH and chitosan: Drug release and mechanism evaluation. *Int. J. Biol. Macromol.* **2019**, *122*, 157–167. [CrossRef]
230. Piao, H.; Kim, M.H.; Cui, M.; Choi, G.; Choy, J.H. Alendronate-anionic clay nanohybrid for enhanced osteogenic proliferation and differentiation. *J. Korean Med. Sci.* **2019**, *34*, e37. [CrossRef]
231. Khorsandi, K.; Hosseinzadeh, R.; Shahidi, F.K. Photodynamic treatment with anionic nanoclays containing curcumin on human triple-negative breast cancer cells: Cellular and biochemical studies. *J. Cell. Biochem.* **2019**, *120*, 4998–5009. [CrossRef]
232. Liu, C.G.; Kankala, R.K.; Liao, H.Y.; Chen, A.Z.; Wang, S.B. Engineered pH-responsive hydrazone-carboxylate complexes-encapsulated 2D matrices for cathepsin-mediated apoptosis in cancer. *J. Biomed. Mater. Res. Part A* **2019**, 1184–1194. [CrossRef]
233. Wen, J.; Yang, K.; Ding, X.; Li, H.; Xu, Y.; Liu, F.; Sun, S. In Situ Formation of Homogeneous Tellurium Nanodots in Paclitaxel-Loaded MgAl Layered Double Hydroxide Gated Mesoporous Silica Nanoparticles for Synergistic Chemo/PDT/PTT Trimode Combinatorial Therapy. *Inorg. Chem.* **2019**, *58*, 2987–2996. [CrossRef]
234. Chakraborty, M.; Mitra, M.K.; Chakraborty, J. One-pot synthesis of CaAl-layered double hydroxide–methotrexate nanohybrid for anticancer application. *Bull. Mater. Sci.* **2017**, *40*, 1203–1211. [CrossRef]
235. Bhattacharjee, A.; Rahaman, S.H.; Saha, S.; Chakraborty, M.; Chakraborty, J. Determination of half maximal inhibitory concentration of CaAl layered double hydroxide on cancer cells and its role in the apoptotic pathway. *Appl. Clay Sci.* **2019**, *168*, 31–35. [CrossRef]
236. Yu, J.; Martin, B.R.; Clearfield, A.; Luo, Z.; Sun, L. One-step direct synthesis of layered double hydroxide single-layer nanosheets. *Nanoscale* **2015**, *7*, 9448–9451. [CrossRef]
237. Weng, Y.; Guan, S.; Lu, H.; Meng, X.; Kaassis, A.Y.; Ren, X.; Qu, X.; Sun, C.; Xie, Z.; Zhou, S. Confinement of carbon dots localizing to the ultrathin layered double hydroxides toward simultaneous triple-mode bioimaging and photothermal therapy. *Talanta* **2018**, *184*, 50–57. [CrossRef]
238. Wang, Z.; Liang, P.; He, X.; Wu, B.; Liu, Q.; Xu, Z.; Wu, H.; Liu, Z.; Qian, Y.; Wang, S.; et al. Etoposide loaded layered double hydroxide nanoparticles reversing chemoresistance and eradicating human glioma stem cells: In vitro and in vivo. *Nanoscale* **2018**, *10*, 13106–13121. [CrossRef]
239. Bouaziz, Z.; Soussan, L.; Janot, J.M.; Jaber, M.; Ben Haj Amara, A.; Balme, S. Dual role of layered double hydroxide nanocomposites on antibacterial activity and degradation of tetracycline and oxytetracyline. *Chemosphere* **2018**, *206*, 175–183. [CrossRef]

240. Asiabi, H.; Yamini, Y.; Alipour, M.; Shamsayei, M.; Hosseinkhani, S. Synthesis and characterization of a novel biocompatible pseudo-hexagonal NaCa-layered double metal hydroxides for smart pH-responsive drug release of dacarbazine and enhanced anticancer activity in malignant melanoma. *Mater. Sci. Eng. C* **2019**, *97*, 96–102. [CrossRef]
241. Shahabadi, N.; Razlansari, M.; Zhaleh, H.; Mansouri, K. Antiproliferative effects of new magnetic pH-responsive drug delivery system composed of Fe_3O_4, CaAl layered double hydroxide and levodopa on melanoma cancer cells. *Mater. Sci. Eng. C* **2019**, *101*, 472–486. [CrossRef]